^{3}HE MELTING CURVE THERMOMETER

by

ICHIRO SHINKODA

B.SC., UNIVERSITY OF BRITISH COLUMBIA, 1981

A THESIS SUBMITTED IN PARTIAL FULFILMENT OF

THE REQUIREMENTS FOR THE DEGREE OF

MASTER OF SCIENCE

in

THE FACULTY OF GRADUATE STUDIES

DEPARTMENT OF PHYSICS

We accept this thesis as conforming

to the required standard

THE UNIVERSITY OF BRITISH COLUMBIA

DECEMBER 1983

In presenting this thesis in partial fulfilment of the requirements for an advanced degree at the University of British Columbia, I agree that the Library shall make it freely available for reference and study. I further agree that permission for extensive copying of this thesis for scholarly purposes may be granted by the Head of my Department or by his or her representatives. It is understood that copying or publication of this thesis for financial gain shall not be allowed without my written permission.

Department of PHYSICS

The University of British Columbia
2075 Wesbrook Place
Vancouver, Canada
V6T 1W5

Date: DECEMBER 30, 1983

Abstract

This thesis decribes the choice, the construction, the operation, and the testing of a ^{3}He melting curve thermometer. The melting curve thermometer satisfies the need of this particular laboratory for a convenient standard thermometer in the temperature range of 6 mK to 600 mK. Over most of its operating range, the resolution of the temperature measured with the ^{3}He melting curve thermometer is 0.03%, however, the accuracy is only 0.3%. The construction of a precision low temperature strain gauge is described. Also a ratio transformer capacitance bridge which has a resolution of 1 ppm is described.

Table of Contents

List of Tables

List of Figures

ACKNOWLEDGEMENTS

I would like to acknowledge the support of Dr. W.N. Hardy in the supervision of this project. I have also benefited from the numerous discussions with B.W. Statt. Also, I would like to thank M. Hurlimann and M.W. Reynolds for their assistance during the running of the experiment. Finally I wish to thank the National Sciences and Engineering Research Council of Canada for a Postgraduate Scholarship.

I. Temperature and Thermometry Below 1K

1.1 Introduction

Accurate measurement of temperatures below 1 K is a very demanding task; as the number of experiments conducted at very low temperatures in different laboratories increases, the demand for standard methods grows. The intercomparision of experimental results which depends on an accurate measurement of the temperature is complicated by the fact that an internationally accepted practical temperature scale has yet to be defined for the temperature range 1 mK to .5 K {the International Practical Temperature Scale (Metrologia, 1979) is presently defined only down to .5 K}. In addition, the physical properties of materials at low temperatures make accurate thermometry extremely difficult at these temperatures.

The purpose of this thesis is to build a ^{3}He melting curve thermometer to serve as a laboratory standard in a temperature range from a few mK to 400 mK(Greywall and Busch, 1982). The ^{3}He melting curve thermometer was chosen for a number of reasons. First of all it has the advantage that it is insensitive to rf, it is insensitive to magnetic fields as large as 5 kG, it has a fast thermal response time, and it dissipates essentially zero power(Greywall and Busch, 1982a). Secondly,

since the ^{3}He melting curve has a well defined minimum in its thermodynamic P-T diagram, once a value has been chosed for the minimum pressure point, every laboratory using a ^{3}He melting curve thermometer can compare the pressure standard used in the lab and apply necessary corrections. Also, the A-transition on the ^{3}He melting curve could in principle be used in conjunction with the minimum point to make the thermometer a self-calibrating system. However, since the A-transition occurs at 2.75 mK, a temperature below the lowest temperature attainable with the present dilution refrigator,it is of no immediate practical interest to this laboratory.

The ^{3}He melting curve thermometer is a temperature standard in the same sense as the He vapour pressure scales are. It is not possible to directly measure the thermodynamic temperature by measuring the pressure, but one relies on the P-T diagram having been previously measured using a primary thermometer.

The rest of the chapter clarifies what is meant by the temperature of a system and describes briefly the physical difficulties one has to master in order to do meaningful thermometry at low temperatures. A brief review of the other thermometers which could be used at temperatures below 1 K is given with an emphasis on the thermal characteristics, rather than the technical aspects of each thermometer. Chapter two considers the theories which are used to describe the melting curve, and summarizes the predictions and measured properties of

the melting curve. The third chapter describes the construction of the thermometer, which is borrowed directly from Greywall and Busch(1982a). The final chapter describes in detail how to utilize the ^{3}He melting curve thermometer to measure temperatures to better than 0.1 mK accuracy at low temperatures.

1.2 Temperature

There exists a physical quantity that describes the thermodynamic state of systems which are in thermal equilibrium with each other. The first postulate of thermodynamics concerns itself with the existence of such a quantity, called temperature. The second law of thermodynamics defines the absolute temperature scale (Reif,1965) of a system by

$$T = \frac{\partial E}{\partial S} , \tag{1}$$

where S is the entropy of the system and E is the internal energy of the system. The partial differentiation is evaluated with all other extrinsic variables of the system held constant.

Practically, the temperature can be measured by observing a physical property of a system which varies reproducibly and monotonically with the temperature. The temperature scale defined by such measurements is an arbitrary empirical scale. A reversible heat engine can be used to relate the thermodymanic temperature scale to a practical temperature scale. If a perfect gas is used as the working substance in a Carnot cycle, it can be shown (Kittel, 1969) that

$$\frac{T_1}{T_2} = \frac{\Theta_1}{\Theta_2} , \tag{2}$$

where T_1 and T_2 are the thermodynamic temperatures at the points in the Carnot cycle, and Θ_1 and Θ_2 are the corresponding temperatures defined by the equation of state of the gas,

$$PV = nR\Theta, \tag{3}$$

where P is the pressure, V is the volume occupied by the gas, R is the molar gas constant, and n is the number of moles of the gas. To prove equation (2) it is necessary to restrict the energy by

$$\left.\frac{\partial E}{\partial V}\right|_{\Theta} = 0. \tag{4}$$

According to equation(2), the thermodynamic temperature scale and the perfect gas temperature scale are identical if both have the same value at one point.

In 1954, the 10th General Conference on Weights and Measures chose 273.16 K for the thermodynamic triple point of water. The value of the gas constant, depends directly on the arbitrary choice of the temperature scale. The equation of state of a non-ideal gas has correction terms to that of the ideal gas, but it may be written in the form

$$PV = nR\Theta + BP + CP^2 + \cdots, \tag{5}$$

where B, C,..., are functions of temperature. Because the correction terms can be calculated to sufficient accuracy, a gas thermometer, where applicable, is used to define the thermodynamic temperature scale.

In the formulation of statistical mechanics of many particle systems, a parameter appears which has the same value for systems in equilibrium with each other. The entire derivation of thermal physics can be accomplished without reference to the thermodynamic temperature(Kittel,1969). If that parameter is postulated to have the role of a temperature, the laws of thermodynamics can be derived from statistical mechanics. A constant can be found that relates the statistical mechanical temperature, τ , with the thermodynamic temperature, T, through,

$$\tau = k T, \tag{6}$$

where k is Boltzmann's constant. Like the gas constant, Boltzmann's constant is not a fundamental constant, as its value depends upon the choice of the temperature scale.

Systems which can be described by statistical mechanics can be used to find the statistical mechanical temperature and by definition the thermodynamic temperature. Two such systems, which can be used for thermometry below 1 K, are the system of weakly interacting paramagnetics and the system of electrons in

a conductor.

1.3 The International Practical Temperature Scale

A gas thermometer measures the thermodynamic temperature, but it is a complicated system; the demands of technology and science require more convenient thermometers. To this end, the Bureau International des Poids et Measures created the IPTS, which has been revised several times. The aim of the IPTS is to furnish a temperature scale which is practical and is as close as possible to the thermodynamic scale.

The latest revision of the IPTS occurred in 1968, and the temperature scale then defined is called the IPTS-68(Metrologia,1969, Preston, 1976). The scale is defined by eleven fixed points, which were assigned the best value of the thermodynamic temperature. The fixed points range from the triple point of hydrogen(13.81 K) to the freezing point of gold(1337.58 K). Furthermore, interpolation formulae are given for stardard specified instruments. The platinum resistance thermometer is used in the range 13.81 K to 630.74 °C, the platinum with 10% rhodium versus platinum thermocouple is used for the region 630.74 °C to 1064.3 °C, and finally the higher temperatures are defined by the Planck law of radiation with 1337.58 K as the reference temperature and a value of 0.01388 mK for C_2, the second radiation constant.

The IPTS-68 deviates from the thermodynamic temperature scale in several places, a summary of which is given by

Hudson(1980). In an effort to correct these deviations and to extend the temperature scale below 30 K, the "1976 Provisional 0.5 K to 30. K Temperature Scale " was defined(Metrologia, 1979). No temperature scale has been defined by the Bureau International des Poids et Measures for temperatures below .5 K.

N.B.S. has defined a scale from 10 mK to .5 K using a nuclear orientation(NO) thermometer of ^{60}Co in a single crystal of ^{57}Co, a Josephson noise thermometer(JNT), and a CMN susceptibitity thermometer calibrated by the NO and JNT(Soulen and Marshak, 1980). Until an international temperature scale for temperatures below .5 K is created, this laboratory will use the scale defined by N.B.S.

1.4 Thermal Properties at Low Temperature

Thermometry below .5K suffers not only from a lack of a well defined scale, but also from technical problems due to physical properties common to all materials at very low temperatures. At very low temperatures the specific heat of all materials become very small, so that a very small heat input drastically changes the temperature of the sample. By arguments identical to the Kinetic theory of gases the conductance, K, can be written as(Kittel,1969)

$$K = \frac{1}{3}\left(\frac{C}{V}\right) l_e v, \tag{7}$$

where (C/V) is the specific heat per unit volume, v is the average speed of the heat carriers, and l_e is their mean free path. At temperatures below 1 K, the mean free path of the carries is determined by the impurity concentration or the sample size. The speed of the carriers is essentially independent of the temperature at these low temperatures. Thus, the thermal conductivity of materials decreases with the temperature. A second source of thermal gradients is the thermal boundary resistance, R_b , often called the Kapitza resistance, between two bodies in thermal contact. To perform accurate and precise temperature measurements on a system, the thermometer must be carefully designed with these obstacles in

mind.

A firm understanding of the thermal properties of materials at temperatures below 1 K is necessary in order to design and install a useful thermometer into a cryogenic system. Here a quick scan of general properties and some common techniques used to reduce thermal gradients are presented, for more detailed information chapter 9 of the book by Lounasmaa is recommended.

In insulators, the heat is transported by phonons. The dominant wavelength , λ , is approximately given by $(\Theta_D/T)d$, where Θ_D is the Debye temperature and d is the lattice spacing. For most elements the Debye temperature is on the order of 100 K or more(Kittel). Thus below 1 K the phonon wavelength is much longer than lattice imperfections and the phonons are not scattered by the imperfections. In the millikelvins, the phonon mean free path, (l_p), is equal to the shortest distance between boundaries. Moreover, as the number of phonons is small there are very few umklapp collisions(Ahshcroft and Mermin, 1976) and so there is no impedance to flow from phonon-phonon interactions. The specific heat of phonons is proportional to T^3, the speed of sound is relatively independent of T, therefore by equation (7) the conductivity is proportional to $l_p T^3$.

In metals, there is additional heat transport by the conduction electrons. At low temperatures the mean free path of electrons is determined by the impurity concentration. The Fermi speed, v, is independent of the temperature and the

specific heat of electron is proportional(Kittel) to T, so that equation (7) gives $K \propto T$. However, the phonons in a metal are scattered by the electrons whose energies lie within kT of the Fermi surface. The number of such electrons is proportional to T, so that the mean free path of phonons is proportional to 1/T. So finally, using equation (7) again the total heat conductance in a metal is given by

$$K = aT + bT^2, \tag{8}$$

where a and b are constants. At very low temperatures all the heat is carried by electons, thus K = aT. The Wiedemann-Franz law(Ashcroft and Mermin)

$$\frac{K}{\sigma} = \frac{\pi^2 k^2}{3e^2} = \mathcal{L} T, \tag{9}$$

where σ is the electrical conductivity, is then valid. The Lorenz constant $\mathcal{L}$ = 25nW /K^2. Equation (9) is often used to calculate the thermal conductivity from the more readily measured electrical conductivity.

The metal with the highest measured thermal conductivity at low temperature is very pure copper(Lounasmaa). The conductivity of all metals can be improved by carefully annealing the sample. To obtain the best results, the annealing process should be the last step before mounting into the

apparatus because copper is readily work hardened. Good thermal conductivity not only in the thermometer but also in the apparatus, whose temperature is being measured, is important if accurate thermometry is desired.

The thermal conductance between two surfaces is found to be proportional to the force pressing the surfaces together(Lounasmaa). The irregularities in the surfaces allow the two surfaces to touch in a small number of high spots and as the pressure is applied these points are deformed until the pressure drops to just below the yield pressure. Thus the surface area in thermal contact is proportional to the applied force and therefore so is the thermal conductance. The thermal resistance between solids made of the same or similiar materials separated by a barrier which is much thinner than the wavelength of the heat carriers is proportional to $1/T$ for metals and $1/T^3$ for dielectrics. Dirty contact between metals which permit only phonons to pass through causes the thermal resistance to be proportional to $1/T^2$, as would be expected from equation(8). The thermal resistance between a metal and a dielectric is proportional to $1/T^3$. All these temperature dependencies have been observed as predicted(Suomi et al, 1968)

As the thermal conductance is proportional to the applied force, two bodies held together by bolts will have a large thermal boundary resistance if the bolts are not tightened with a large torque. If good metal to metal contact cannot be made,

a large thermal boundary resistance can be avoided by using a very thin layer of bonding agent to provide more thermal contact between the bodies. Apiezon N, General Electric 7031 varnish, and Epibond 121 have been used for this purpose(Anderson and Peterson, 1970). The most effective method for minimizing the thermal boundary resistance is to solder the two pieces together with a nonsuperconductiong solder. But, when this is not possible and the pieces must be readily demountable, some effort should be put into gold plating all the metal pieces. Furthermore, the thermal contraction of the apparatus pieces must be carefully taken into account when using bolts. Sometimes, the differential thermal contraction can be used to provide a large force.

The term Kapitza resistance is often restricted to mean the thermal boundary resistance between liquid helium and a solid body. The nature of the boundary resistance is not theoretically well understood(Lounasmaa), although much study has been done(Keller,1969). A comprehensive review of the Kapitza resistance of helium and various solids was compiled by Harrison(1979).

The Kapitza resistance is very sensitive to the surface condition of the solid. A copper sample carefully annealed in a vacuum will have a Kapitza resistance an order of magnitude greater than a similiar untreated piece. Further, the Kapitza resistance of the treated sample can then be decreased by 30% by

wiping the surface with a tissue(Lounasmaa). The Kapitza resistivity , defined by $r = R_B A$, where R_B is the Kapitza resistance and A is the surface area in thermal contact, is approximately the same within a factor of three between liquid ^3He, liquid ^4He, or dilute mixtures of ^3He in ^4He, and a metal or an insulator. The product $R_B T^3$ is approximately constant below 0.1 K , increases by an order of magnitude between 0.1 and 0.7 K, and then is approximately constant above 0.7 K.

A standard method of decreasing the Kapitza resistance is to increase the surface area in contact with the liquid using a sinter made of copper or silver. Properly sintered silver powder of 700A diameter particles has a surface area of a meter squared per gram of sinter.(Harrison, 1979). More information about sinters will be given in chapter 3, when the construction of the ^3He cell is described.

1.5 Review of Practical Thermometers Below 1 K

Thermometers are classified according to the extent they are capable of measuring the thermodynamic temperature. The primary thermometers are the class of thermometers which can determine the thermodynamic temperature without any previous knowledge of the temperature in the region of interest. Secondary thermometers, however, require that they be calibrated against a primary thermometer before they can be used to measure the thermodynamic temperature. There exists a third class of thermometers, which will be called secondary standards, although most review articles(Lounasmaa, Hudson et al) include them under the classification of primary thermometers. A secondary standard thermometers must be calibrated by a primary thermometer before it can measure the absolute temperature. Because the physical quantity measured by the thermometer was chosen for the reason that it is independent of the sample, once a particular secondary thermometer is calibrated, all others of the same type are also calibrated. Examples of secondary thermometers are the ^{3}He vapour pressure, the superconducting fixed point, and the ^{3}He melting curve thermometers.

One may be tempted to use only primary thermometers in an experiment to achieve accurate thermometry, but such experiments would be very tedious. The disadvantage of primary thermometers is that they are complicated and require substantial time per

measurement. The secondary thermometers are simple to implement and require only a few seconds per temperature measurement. The major disadvantage with secondary thermometers is the possibility that the calibration may change when the device is repeatedly cooled to low temperature. The secondary standards have the problem that they are difficult to implement and require several minutes per measurement, but they are more convenient to use than the primary thermometers.

The rest of the chapter is devoted to a review of the merits of various thermometers. The secondary thermometers which are discussed are resistance, paramagnetic susceptibility, and nuclear magnetic resonance thermometers. The ^{3}He and ^{4}He vapour pressure, the ^{3}He melting curve, and the superconducting fixed point are secondary standards covered in this thesis. Finally, the osmotic pressure, the noise, the nuclear orientation, and the Mossbauer thermometers are primary thermometers which are discussed.

1.5.1 Resistance Thermometry

The most common thermometers at cryogenic temperatures are resistance thermometers, because they are relatively easy to obtain, and are compact and easy to operate. Although these thermometers are the most versattile temperature sensors at low temperature, only a very brief discussion is given here.

Phosphorus or arsenic doped germanium resistors are used as thermometers because their calibration is stable to better than 1 mK over long periods of time. The advantage of a germanium resistor is that once it has been calibrated, it may be used as a temperature standard. Commerical germanium reisitors are available which can be used down to 50 mK.

The most common resistance thermometer sensors are carbon composition resistors. They have the advantage that they much less expensive than the germanium resistors. Carbon resistors are insensitive to radiation or external pressure, but are sensitive to magnetic fields. The magnetoresistance effect increases with the temperature sensitivity of the resistor, so that the temperature error is approximately constant or slightly increases at lower temperatures. The magnetoresistance of an individual resistor is difficult to accurately predict, but a typical value is 1% change in the apparent temperature per 1 T(Lounasmaa).

The resistors most commonly used for thermometry below 1 K

are Speer(Grade 1001)(Edelstein and Mess,1965) and Matsushita(ERC-18GJ)(Saito and Sato, 1975). The Matsushitas are preferred at the lower temperatures because they have a smaller specific heat and are easier to thermally ground than Speers. The one major disadvantage with resistance thermometers is that they are secondary thermometers and thus need to be calibrated. The calibration of a typical resistor can change a few percent as it is repeatedly cycled. The accurate calibration of thermometers is a difficult task that requires a great deal of thought and hard work. In this laboratory it has been found that commerically calibrated devices cannot be completely trusted and should be checked against other temperature standards.

When measuring temperatures below 100 mK, care must be taken to ensure that the resistor is in good thermal contact with the thermal bath. Usually the resistors are ground to a thin waffer and then mounted in a gold plated holder to achieve good thermal contact (Robichaux and Anderson, 1969). Similiarly, the leads to the resistor should be carefully thermally anchored. When attaching leads to a resistor it should be remembered that heating a carbon resistor can change its calibration.

Rf pickup in the leads attached to resistors can cause heating of the resistor; this can be quite substantial below 50 mK. If an electrically shielded room is not available, low

pass filters to ground should be attached to all leads going into the cryostat. Most resistance bridges use low a.c. excitation voltages so that thermal emf and spurious emf induced by moving leads does not affect the measurement of the resistance. When sufficient precautions are taken, the resistor thermometer can be used to measure temperatures down to 3 mK(Lounasmaa)

A useful "rule of thumb" is that the power dissipated in a carbon resistor by the resistance bridge should be less than $\dot{Q} = T^3nW/K^3$, if the accuracy, $\delta T/T$, of the temperature measured is to be better than 10^{-4}(Lounasmaa).

1.5.2 Paramagnetic Thermometry

The paramagnetic susceptibility, χ, of a system of non-interacting magnetic dipoles is described by the Curie law

$$\chi = \frac{c}{T} \quad (10)$$

where c is the Curie constant. In principle, the susceptibility of a dilute system of paramagnets could be used for absolute thermometry, but because the measured susceptibility depends on many factors such as the material, the shape of the sample, and the contributions from impurities, it is instead used as a good secondary thermometer. If nearest neighbour dipole-dipole interactions are taken into account, equation (10) is modified into the Curie Weiss law

$$\chi = \frac{c}{T-\theta} \quad (11)$$

where θ is the Weiss constant. The Curie Weiss law has two constants, thus only two fixed points are necessary to calibrate the thermometer, but for very precise work several fixed points are used to determine the constants.

The most suitable paramagnetic salt for thermometry(Soulen, 1982) is a single crystal of cerium magnesium nitrate (CMN). This material has been extensively studied(Zimmerman et al,

1980) and shown to obey the Curie law down to 50 mK. A single crystal of CMN loses thermal contact with the enviroment below 30 mK. The thermal boundary resistance can be reduced by using powdered CMN in a slurry of grease and copper wires or in liquid ^{3}He(Wheatly, 1975, Richardson, 1977). Although no careful thermodynamic studies have been done on powdered CMN, comparison(Abesbourne et al, 1973) of a single crystal and a powder of CMN fitting in a right circular cylinder with the diameter equal to the height have shown agreement within 0.05 mK at 3 mK. The susceptibility of the powder is well described(Wheatly, 1975) down to 2 mK by

$$\chi = \frac{c}{T - \theta} + B, \qquad (12)$$

where B is a constant. At very low temperatures, the thermal time constant of a slurry of CMN and grease shows an increase as T^{-3} and at 8 mK is 40 minutes(Greywall and Busch, 1982a). Below a few mK the dipole-dipole interactions become large so that the measured susceptibility deviates from the Curie Weiss law. These two facts limit the lowest temperature that can be measured with a CMN thermometer.

A thermometer using lanthanum diluted CMN(LCMN) has a smaller molar heat capacity(Hudson et al). Because the concentration of the paramagnetic ion is less in the LCMN, the dipole interactions are less significant, so LCMN can be used to

lower temperatures than CMN. The susceptibility of the LCMN has been measured(Wheatly, 1975) and shown to obey (12). The thermal time constant of LCMN has been measured for LCMN in ^3He and found to be roughly constant at 7 minutes for temperatures between 20 mK and 8 mK.

The susceptibility of the paramagnetic sensor is usually measured by placing the salt in one of a pair of astatically wound coils and then measuring the mutual inductance of the system as a function of the temperature. Traditionally, the mutual inductance was measured using a ratio transformer and a low audio frequency (20-300 Hz) excitation voltage, but for low temperatures squid magnetometers have almost completely replaced the ratio transformer system. The advantage of a squid is that the system requires only 1/1000 of the sensor material for the same sensitivity as the ratio transformer system. The disadvantages of the squid magnetometer thermometer are that a small d.c. field is required to bias the salt and the astatic coils must be well shielded from ambient magnetic noise.

In summary, the susceptibility thermometer using a single crystal of CMN is a good thermometer in the range 30 mK to 30 K. If the thermometer is to be used below 1 K, then the thermometer must be calibrated at points below 1 K. A thermometer calibrated only at the higher temperatures is not a reliable thermometer for temperatures below 1 K. In the millikelvin range, the thermometer can easily achieve a resolution of a few

microkelvin. At the very low mK range powdered CMN or LCMN in a slurry of grease of ^{3}He can be used to measure temperatures down to 2 mK.

1.5.3 Nuclear Magnetic Thermometry

Nuclear paramagnetism can be used to measure the temperature by methods similiar to that used for electronic paramagnetic thermometers. The advantage of using nuclear magnetic moments is that they obey the Curie law down to temperatures in the microkelvins. The Weiss constant can be of the order of a few microkelvins. The preceding is strictly true for zero external fields. In a finite external field the corrections to the series expansion of the Brillouin function is of the order B^2T^2. For copper at 1 mK and 0.2 T, the correction is less than 1%. The nuclear magnetic thermometer(NMT) would be a good primary thermometer except that the effective Curie constant cannot be accurately calculated for the experimental situations,thus the, NMT is a secondary thermometer. The disadvantage of using the nuclear magnetic moments is that the magnetic moments are much smaller than the electronic paramgnetic moments.

The sensor material must satisfy several conditions. The Weiss constant will be of the order of microKelvin only if two constraints are met. If the nuclear spin, I, is greater than 1/2, then the site symmetry of the nucleus must be cubic otherwise there will be splitting of the nuclear spin energy levels due to the electric field gradients. This splitting can be as large as 0.01 K. The second requirement is that the

material should not be magnetically ordered, as the local magnetic field would then be the sum of an applied field and an internal magnetic field and thus Curie's law would not apply to the applied magnetic field. A NMT measures the nuclear spin temperature which is not necessarily the same as the lattice temperature. The sensor must therefore posses a short relaxation time, T_1 , between the nuclear spin and the lattice. The T_1 for metals are orders of magnitude shorter than the T_1 of diamagnetic insulators. The T_1 and the conduction electron temperature, which is the lattice temperature of a metal, are related by the Korringa relation

$$T = \frac{b}{T_1} \quad (13)$$

where b is a constant. The constant has been measured(Hudson et al) for several metals and is 1.27 Ksec(Anderson and Redfield, 1959) for copper and 0.0296 Ksec for platinium. The requirement there be good thermal contact between the sensor and the temperature bath necessites the use of a metal for the sensor element. The metal must be available in very pure form and must not be superconducting during the measurement. The nuclei of interest should have high natural abundance and a large gyromagetic ratio so that the Curie constant will be large. The two most common metals which are used as the sensor elements of a NMT are copper and platinium(Richard et al, 1973, Dundon et

al, 1973).

Although the NMT is a secondary thermometer, it is possible to self-calibrate the thermometer using the Korringa relation, but the accuracy is usually only of the order of 3%(Hudson et al). The susceptibility of the sensor can be measured by nonresonant or resonant techniques.

The susceptibility of the sensor material in a small applied magnetic field is measured by methods identical to that used in electronic paramagnetic thermometers and the temperature inferred using Curie's law. The major difficulty in implementing a static NMT is that the electronic magnetization due to the impurties in concentrations 1 ppm can be equal to the nuclear contribution to the measured magnetization. A solution to this problem is to saturate the electronic contribution by applying a large magnetic field or to calibrate the system at a low enough temperature so that the electronic magetization is fully saturated. A problem with applying a large magnetic field is that the lifting of the nuclear state degeneracies increases the nuclear spin heat capacity, thus increasing the thermal equilibrium relaxation time. For example, at 10 mK the nuclear and electronic heat capacities of copper are equal in a magnetic field of 145 G(Hudson et al).

Until the developement of the Squid magnetometer, the sensitivity of the static measurement was less than that achievable by resonant methods. The Squid magnetometer is

usually used (Bubrman et al, 1971) to measure the magnetization of the sample in a small magnetic field (100 G). The resolution of a typical system is given by

$$\frac{\Delta T}{T} = \frac{5 \times 10^{-2}}{B} \text{ gauss} . \tag{14}$$

At T =10mK and B = 10 G, it is possible to resolve 50 uK. The accuracy of the temperature is determined by the calibration and is usually worse than 1% (Hudson et al). The advantage of the static method over the resonant techniques for measuring the magnetization of the sensor material is that very little energy is absorbed by the thermometer during the measurement. The heating in the nonresonant system is due to noise generated eddy currents. It has been estimated(Hirschkoff et al, 1970) that the temperature rise will be 1% at 1 mK in copper wires of 2.3 x 10^{-3} mm diameter assuming a R.F. squid operting at 190 MHz and a magnetic flux fluctuation of one fluxon.

The nuclear magnetization can also be measured by two different resonant methods. The first method is a pulsed nuclear magnetic resonance(NMR) technique and the second is a continuous wave(CW) resonance techuique. The advantage of a resonance measurement of the magnetization is that the electronic impurities, with Lamor frequency a thousand times larger, do not contribute to the measured magnetization. They may, however, distort the local field and broaden the line width

of the signal.

The NMR technique measures the magnetization of the nuclei by measuring the free induction decay (FID) of the sample. Because standard NMR techniques are used to measure the magnetization, the NMR apparatus will not be described here. The magnetizaion of a sample in a steady field, B_o, in the z-direction is tipped by a small angle by applying a magnetic pulse $B\cos(\omega t)$ for a time, t, where ω is the Lamor frequency of the nucleus in B_o. Because the thermal capacity of the nuclear spin system is proportional B_o^2(Hudson et al) , it is desirable to keep B as small as possible(usually of the order of a 10 G). The magnetic component in the x-direction is $M\sin\theta$, this precesses at the Lamor frequency around the z-axis. A voltage is which is proportional to $M\sin\theta$ is induced in a loop perpendicular to both B_o and the x-axis. The induced voltage decays in a time determined by the spin-spin relaxation time, T_2, and the inhomogeneity of the steady magnetic field. The induced voltage is proportional to 1/T through the magnetization. Small tipping angles must be used because decreasing the magnetization along B_o from M to $M\cos\theta$ increases the temperature of the spins from T to $T/\cos\theta$. This reduces the induced voltage, but because at low temperature the FID signals are large, small tipping angles are adequate. Further, the pulsed NMR technique measures the nuclear magnetization before the tipping pulse, thus the temperature of the nucleus before

the temperature increase is measured. If the spin-lattice relaxation time, T_1, is short, then the pulsed NMR method measures equilibrium temperature of the sample, which is unaffected by the transients caused by the pulse. Because at temperatures below 1 K platinium has a T_2 of 1 msec compared to copper with a T_2 of 80 sec and a much shorter T_1 than the copper, platinium is the best choice. Care must be taken when using platinium because impurities can make Curie's law invalid for a particular specimen.

The pulsed NMR thermometer can be made self-calibrating by first measuring T_1 by destroying the magnetization in the B direction by a $\pi/2$ pulse and observing the time for the magnetization to return to equilibrium. Then Korringa's relation is used to find the electronic temperature.

The major source of self-heating in the thermometer is the eddy current heating in the sensor. For a cylindrical conductor of radius r, volume V, resistivity R, and in a changing magnetic field B along the direction of its axis assuming full penetration of the field, the eddy current heating(Lounasmaa) is

$$\dot{Q} = \frac{r^2 V}{8R} \left(\frac{dB}{dt}\right)^2 . \tag{15}$$

In the range of a few mK to 4 K, the precision of the temperature measured with the pulsed NMR is about 0.5% with an

absolute accuracy of 2% depending on the calibration used(Anufrieu and Peshor,1972). A NMR thermometer self-calibrated using the Korringa relation has an accuracy of about 3%(Hudson et al).

The second resonant method is continuous wave NMR (CW). The sensor sample is placed in a high, steady magnetic field $B_z = B_o$ and is radiated with a much smaller $B_y = B \sin\omega t$ at right angle to B_z. The transverse susceptibility, $\chi = \chi' - i\chi''$, of the sample is described by the Bloch equation. Either the real or imaginary part may be measured by CW and used for thermometry. The imaginary part of the susceptibility, χ'', can be measured by detecting the energy absorbed for the magnetic field by the nuclear spin system, and the real part of the susceptibility, χ', can be measured by observing the voltage induced in a coil perpendicular to both the z and y axis by the rotating nuclear magnetization induced by B_y.

The power absorbed by the spins from the radiofrequency field is given by $\dot{Q} = \omega\chi''B^2/2$ and can be measured in an NMR experiment. Because the CW method is constantly injecting energy into the spin system, if T_1 is too long, the temperature of the spin system can be be higher than the temperature of the lattice.

1.5.3 Vapour Pressure Thermometry

The vapour pressure thermometer is not a primary thermometer in the sense that another primary thermometer is required to measure the latent heat of vapourization and the boiling point or to measure the vapour pressure as a function of the temperature. Once these values are tabulated the vapour pressure can be used to find the temperature of a system. When measuring temperatures to high accuracy the tabulated values of temperature versus the vapour pressure are used, rather than the thermodynamic vapour pressure-temperature relation (Dijk and Durieux, 1958) for a monatomic vapour gas given by

$$(20) \qquad \ln(P) = -\frac{L_o}{RT} + \frac{5}{2}\ln(T) + i_o + \varepsilon(T) + \frac{1}{RT}\int_o^P v_\ell \, dP - \frac{1}{RT}\int_o^T s_\ell \, dT,$$

where L_o is the heat of vaporization at $T = 0$, R is the molar gas constant, and $i_o = \ln[(2\,m)^{3/2}K^{5/2}/h^3]$ is the chemical constant of the gas. $\varepsilon(T) = \ln[PV_g/RT] - \frac{3B}{V_g} - \frac{3C}{V_g}$ is a correction term representing the non-ideality of the vapour and the last two terms contain integrals of the molar entropy, s_ℓ, and the molar volume of the liquid, v_ℓ, along the saturation curve. The accuracy of the thermodynamic relation depends on how accurately the last three correction terms can be obtained from experimental data. The latent heat at $T = 0$ is determined by fitting equation(20) to the experimental P-T data. Because the

magnitude of the corrrection terms decrease with deceasing temperature (20) may be used for low tempertures. For example, with ^{4}He equation (20) may be used for the calculation of T up to 1.5K with an accuracy of 0.2 mK(Durieux et al,). In the case of ^{3}He, the large liquid contributions makes it preferable to use tables to as low temperature as possible. For low temperatures ^{3}He is preferable to ^{4}He because there is no superfluid film. Below 1.3 K for ^{4}He and 0.7 K for ^{3}He correction for the pressure head in the sensing tube and thermomolecular pressure effect (Greywall and Busch, 1980) must be made. The first correction is of the order of 1 mK and can be easily calculated or measured during the experiment. The size of the thermomolecular pressure correction depends on the size of the sensing tube down into the cryostat and can be as high as a 17 mK correction at .5 K for a tube with a diameter of 2mm and the top end at 293 K.

The capacitance pressure gauge of Gonano and Adams(1970) measures the vapour pressure in situ and avoids the necessity of making any correction to the measured pressure. Such a thermometer with ^{3}He can be used down to 0.3 K with an accuracy of 1%(Lounasmaa).

When using a vapour pressure thermometer it is important to remember that the vapour is in equilibrium with the liquid when the system is cooled and the vapour pressure can be used to find the temperature of the liquid. But, when warming up, the

temperature of the vapour is different from the temperature of the liquid. Furthermore, the temperature of the vapour-liquid interface is not the temperature of the liquid below the surface. Due to the weight of the liquid above it, the temperature of the liquid below the surface is higher than the temperature at the surface.

One note of warning, the ^{4}He vapour pressure scale(T58) has been found to be incorrect(Brickledde et al, 1960) giving temperatures which are everywhere too low by 2%. Similiarly the ^{3}He scale(T62) is incorrect as it had been forced to agree with the T58. The corrected vapour pressured values are given by the T76 tables(Metrologia, 1979).

1.5.5 Fixed Point Devices

A critical point can be used as a reference temperature device once its behaviour is well understood. At temperatures less than 0.5 K, the superconducting phase transition in metals is the most common critical phenomenon. Not all superconductors, however, are useful as fixed point devices. Only metals with sharp transitions, very little hysteresis, and a minimun of supercooling are acceptable for thermometry purposes. The difficulty with using superconducting fixed point device to define the temperature scale is that the transition temperature, T_c, of different samples of the same material can vary as much as 1 mK. The possibility of different transition temperatures requires that one laboratory be chosen to calibrate every superconducting device. Furthermore, the reproducibility of the T in a given sample is only ± 0.1 mK (NBS 260-62).

An ambient magnetic field degrades the performance of the superconducting fixed point device in two ways. First, there is the familiar depression of the transition temperature by a magnetic field. The temperature at which the transition occurs in an ambient magnetic field $H_c(T)$, is related to the critical magneic field, $H_c(0)$, and the zero magnetic field critical temperature, T_c, by

$$H_c(T) \cong H_c(0)\left(1 - \left(\frac{T}{T_c}\right)^2\right) . \qquad (21)$$

Equation (21) can be solved for T. By applying a known magnetic field, temperatures which are a few mK lower than T_c can be measured using the fixed point device. The BCS theory gives a more exact relation than equation (21) and could be used if higher precision is required.

The second effect of the ambient magnetic field is to cause the superconductor to supercool. When a superconductor supercools due to a magnetic field, H, the sample must be cooled considerably below the $T_c(H)$ before it can become superconducting. The maximum depression of T_c due to supercooling can be calculated using the Ginzberg-Landau theory(NBS). Practically, the supercooling hysteresis can be diminished by spotwelding materials with higher T_c to the sensor materials. The spotwelded material acts as a nucleation site and promotes the superconducting transition.

The supercooling effect is always greater than the depression of T_c due to the magnetic field. For a superconducting fixed point thermometer to perform satisfactorily, the maximum ambient magnetic field should be less than 10 mG(NBS). When superconducting magnetic shielding is employed care must be taken to ensure that large magnetic fields(20G) are not generated due to differential cooling of the shield through the transition temperature.

The National Bureau of Standards manufactures a

superconducting fixed point device called the SRM 768 for temperatures below O.5 K. It consists of five superconductors(AuIn , AuAl, In, Be, and W) which have transiton temperatures near 0.208 K, 0.161 K, 0.099 K, 0.024 K and 0.015 K respectively, and an assembly of coils. The mutual inductance between the primary coil and 5 counterwound secondary coils are used to detect the superconducting transitions.

The SRM 768's are calibrated against a gamma-ray anisotropy thermometer and a Josephson junction noise thermometer. The temperature scale used is claimed to coincide with the absolute temperature scale to within a few tenths of a percent throughout the range(NBS).

The accuracy of the temperature measured is seriously affected by the ambient magnetic field as already discussed. It is also affected by the self-heating of the superconducting fixed point device. The a.c. excitation voltage used to measure the mutual inductance of the coils induces eddy current heating in the samples and the sample holders. The requirement that the self-heating be small imposes a compromise in the frequency and amplitude of the excitation signal used, but this restriction is not a serious obstacle in the implementation. The estimated power dissipation in the SRM 768 is 8×10^{-11} watts, when an excitation current of 29 uA at a frequency of 400 Hz is used.

1.5.6 ^{3}He Melting Curve Thermometry

The melting curve of ^{3}He has two distinct features: a minimum in the pressure at T = .32 K and a discontinous change in the slope at the superfluild A transiton at a temperature of 2.75 mK(Greywall and Busch). These features make the ^{3}He melting curve themometer(MCT) a very useful one for comparing laboratory temperature scales. Once the pressure of the two points are assigned, any linear pressure gauge may be calibrated against the melting curve. The MCT would then be independent of the individual lab pressure standard. Even if only one point were to be used, slight corrections to the pressure scale of the lab could be made. The Clausius-Clapeyron equation for the equilibrium melting pressure curve can be applied to the ^{3}He melting curve

$$\frac{dP_m}{dS} = \frac{S_\ell - S_S}{V_\ell - V_S} \quad , \tag{23}$$

where Pm is the melting pressure, S_ℓ and S_S are the molar entropies of the liquid and solid, respectively, and v_ℓ and v_S are the molar volumes of the liquid and the solid at melting. If theoretical expressions for the entropies and the volumes could be derived, then integration of equation(23) would give $P_m(T)$. The MCT would then be a primary themometer. Some progress has been made in the understanding of ^{3}He(Keller), but

much still remains a mystery. Some of the theories and some of the predictions made about the behaviour of the melting curve will be presented in chapter 2. The alternatives are to measure the melting curve using another primary thermometer or to derive the melting curve from measured values of the quantities in equation (23)(Hudson et al). To date, the only method which allows the MCT to give temperature in the range 0.3 K to 2 mK with an accuracy of 1%, is to directly calibrate the ^{3}He melting curve (Greywall and Busch,1982a) against other primary thermometers.

The MCT measures the pressure of a constant number of ^{3}He atoms in a fixed volume as the temperature is changed. A MCT consists of a low temperature pressure transducer, with a constant volume cell for the ^{3}He, a room temperature pressure standard, and a system for compressing the very pure ^{3}He to the required pressures. The ^{3}He cell is closed by a plug of ^{3}He that forms in a section of the capillary at a higher temperature than the cell. The blocked-capillary method(Webb et al,1952), which will be discussed further in chapter four. The trapped ^{3}He then traces out the melting curve as the temperature is varied. Because the mixture follows the melting curve, the pressure of the system can be used to find the temperature. The pressure must be measured in situ because the blocked capillary prevents the pressure variation from being transmitted up the capillary.

Although some commerical transducers can be used to measure the pressure(Weinstock et al, 1962), they tend to dissipate large amounts of heat. The most common method is to use a capacitive pressure transducer of the Straty-Adam type(Straty and Adam, 1969). The capacitive transducer ulitilizes a wall or walls of a container, usually made of Berylco 25 (Corruccini and Mountfield, 1978), to vary the separation of two well defined capacitor plates. The change in capacitance is measured by using the 3-wire guarded ground technique, which detects only the capacitance between the plates and is only slightly affected by the lead capacitance. The diaphragm wall and the capacitor separation are chosen to opimitize the pressure sensitivity of the transducer in the range of interest(Straty and Adam, 1969). The ^{3}He cell must be calibrated with a pressure standard, before it can be used as a thermometer. As the absolute accuracy of the MCT can be limited by the uncertainty in the cell calibration, the pressure standard for the system must be choosen with some care.

The capacitance can be measured to $\Delta C/C = 10^{-8}$ using a General Radio Co. Type 1620-A capacitance bridge. The corresponding pressure resolution can be about 5×10^{-6} bar at 30 bars(Greywall and Busch, 1982a).

The ^{3}He is compressed to the required pressures using a charcoal pump(Lounasmaa) or a toepler pump(Johnson and

Wheatley,1970). The impurity level of ^{4}He in the ^{3}He must be kept below 600 ppm (Scribner et al, 1969) and is usually < 20 ppm(Greywall and Busch,1982a).

Many of the advantages of the MCT have been already listed and will not be reiterated, but one further advantage of the MCT is that when better measurements of the melting curve are made, the temperatures measured using the MCT can be easily adjusted to the new calibration.

1.5.7 Osmotic Pressure Thermometry

The pressure difference, P, between a dilute mixture of ^3He in ^4He and ^4He liquid at T = 0 connected by a superleak is given(Lounasmaa) by

$$P = \frac{1}{V_4} \int_0^{X_0} \frac{X_0}{1 - X_0} \left. \frac{\partial \mu_{3,0}}{\partial X_0} \right|_{P,T} dX_0 + \frac{1}{V_4} \int_0^T S_4 \, dT, \qquad (22)$$

where X_0 is the molar concentration of $^3He = n_3/(n_3 + n_4)$, v_4 is the molar volume of pure ^4He liquid, $\mu_{3,0}$ is the chemical potential of ^3He in ^4He and s is the molar entropy of pure ^4He liquid. The first term of equation (22) is the osmotic pressure of ^3He in ^4He, and the second term is called the fountian pressure of ^4He. The behaviour of ^3He molecules in ^4He can be described accurately by treating ^3He as quasi-particles with Fermi statistics.(Landau et al, 1970) Complete analytical expressions are available for the osmotic pressure of ^3He in ^4He over the whole temperature range and concentrations.

The osmotic pressure thermometer is a primary themometer once the density of ^3He in ^4He is known, otherwise the thermometer can be used to extrapolate the ^3He temperature scale down into the millikelvin range. When the thermometer is used as a transfer device, the concentration, x_0, need only be known to within 10%(Rosenbaum et al, 1977). The osmotic pressure thermometer is useful for experiments which study the properties

of ^3He in ^4He. Furthermore, this thermometer has the advantage that it is insensitive to large magnetic fields.

There has been no intensive interest in refining the osmotic pressure thermometer, but the thermometers that have been used have encouraging characteristics. One thermometer has been developed(Bloyet et al, 1975) for thermometry in the range 50 mK to 500 mK with a resolution of 10 uK and an accuracy of 2 mK. The thermometer consists of a capillary with one end in the mixing chamber and a bulb on the other end. A heater on the bulb drives away the ^3He and attracts the superfuild ^4He. The heater supplies a very small amount of power so that the temperature of the bulb is independent of the heater power. The bulb is above the mixing chamber so that the osmotic pressure tries to push ^3He into the bulb, but the heater drives the ^3He away, so temperature of the bulb increases until osmotic pressure on the ^3He in the bulb is equal to the osmotic pressure at the mixing chamber. The pressure balance between the bulb and the chamber defines a relationship between the temperature of the two volumes. A thermometer is used to measure the temperature of the bulb and infers the temperature of the chamber. Thus this thermometer measures a low temperature by measuring a temperature an order of magnitude larger. The higher temperature can be measured by using a ^3He vapour thermometer.

A second thermometer(Lounasmaa) infers the temperature by

measuring the pressure given by equation(22). A small cylindrical reservoir of pure ^{4}He is connected by a superleak to a large chamber containing dilute ^{3}He(x_o = 0.0004 - 0.006) which is at the same temperature as the ^{4}He cylinder. A capacitance technique is used to measure the height of the ^{4}He head in the cylinder and thus the pressure can be inferred. The cross-sectional area of the ^{4}He reservoir is made to be much smaller than that of the dilute ^{3}He reservoir so that the molar concentration of the ^{3}He remains constant to better than 1% as the fliud levels change. A thermometer with x = 0.0004 is useful in the region 20 to 700 mK with an accuracy of 0.2 mK.

In summary the osmotic pressure thermometer can be a very useful thermometer in experiments on properties of dilute ^{3}He in ^{4}He, but much more developement is necessary before it can be used as a reliable general purpose primary thermometer.

1.5.8 Mossbauer Effect Thermometry

Unlike the vapour pressre thermometer, the Mossbauer effect thermometer does not require any direct knowledge of the absolute temperature scale to initially calibrate the system. The Mossbauer effect is the recoilless emission or absorption of -radiation by the nuclei. The lattice in which the nuclei is embedded absorbs the momentum, but absorbs very little energy since the effective mass is essentially infinite. The Mossbauer themometer requires a source and an absorber to radiate and absorb the γ-radiation respectively. Either the source or the absorber can be at the temperature of interest.

Usually the cold absorber thermometer is used because this arrangement is self-calibrating. Here only the cold-absorber thermometer is considered. For details about source thermometry and Mossbauer thermometry in general the paper by Kalius et al(1969) is recommended.

The cold absorber Mossbauer thermometer measures the Boltzmann distribution of the nuclear hyperfine states and thus measures the temperature of the spin system. The γ-ray from an appropriate source is resonantly absorbed and excites the absorbing nuclei from the ground state I_g, to the first excited state I_e. The hyperfine interaction splits the I_g and I_e into hyperfine sublevels, so that the transitions occur between two sublevels m_g and m_e in I_g and I_e respectively. For thin

absorbers the relative transitions in the Mossbauer spectrum is given by

$$R(m_g \rightarrow m_e) = \alpha \rho(m_g)\, C(m_g, m_e), \tag{24}$$

where α is a constant for a given experiment, $C(m_g,m_e)$ is the square of the appropriately normalized Clebsch-Gordon coefficient, and $\rho(m_g)$ is the probability of the system existing in a sublevel m_g calculated assuming the nuclei are non-interacting spin particles in a magnetic field. As the host lattice is doped with only 1% of the Mossbauer effect nucleus and the direct interactions are nuclei - nuclei, this is a good approximation. The probability is calculated as usual by

$$\rho(m) = \frac{N \exp[m \mu_n g_n B/kT]}{\sum_{m'=-I}^{I} \exp[m' \mu_n g_n B/kT]}, \tag{25}$$

where u_n is the nuclear magnetron, g_n is the nuclear g-factor, N is the total number of Mossbauer nuclei in the sample, and B is the local magnetic field. There is one unknown constant in equation (24), but if the nuclear states have a small number of sublevels then α need not be known. As an example, consider the case $I_g = 3/2^+$ and $I_e = 1/2^+$. Then recalling the Clebsch-Gordan coeffiecients have the property that $C(m_g,m_e) = C(-m_g,-m_e)$ and then taking the ratio of the intensities of the two possible transitions one gets,

$$(26) \qquad r = \frac{R(+3/2 \rightarrow +1/2)}{R(-3/2 \rightarrow -1/2)} = \frac{\rho(+3/2)}{\rho(-3/2)} = \exp\left[-3\Delta\epsilon/kT\right] ,$$

where $\Delta\epsilon = -\mu_n g_n B$. By measuring the resonance line separation, $\Delta\epsilon$ can be independently determined. Once $\Delta\epsilon$ is measured the thermometer is calibrated.

The most common Mossbauer isotropes ^{57}Fe and ^{197}Au have $\Delta\epsilon/k$ of 4 mK and 14 mK respectively, so that thermometers with sensory elements made from these are effective thermometers from 2 mK to 20 mK with ^{57}Fe and 7 mK to 50 mK with ^{197}Au(Lounasmaa). The accuracy of the thermometer is determined by the total number of events in the Mossbauer spectrum. The major disadvantage of this thermometer is the large counting time needed for accurate temperature measurement. The Mossbauer thermometer requires the absorption of γ-rays and ,as such, the self-heating of the sensor becomes the limiting factor in the usefulness at the lower temperatures. The technical implementation of a Mossbauer thermometer is a very difficult problem and the added feature of very long measuring times severely limits the use of this thermometer.

1.5.9 Nuclear Orientation Thermometry

If the polarization of a nuclear spin system can be measured, then the absolute temperature can be deduced via the Boltzman factor. There are several methods for measuring the degree of ordering in the nuclear spins, but the only method extensively used for absolute thermometry(Marshak, 1982) at low temperatures is the measurement of the γ-ray anisotropy from decaying nuclei oriented in a magnetic field. The anisotropic emission of γ-rays from oriented radioactive nuclei is well understood(Krane et al, 1973), thus the nuclear orientation thermometer(NOT) can be used as a primary thermometer(Berglund et al, 1972).

Oriented nuclear spin systems with axial symmetry have a normalized spatial distribution, $W(\theta)$, of emitted γ-rays given by

$$(27) \qquad W(\theta) = \sum_{k\,\text{even}} B_k(T)\, R_k\, U_k\, P_k(\cos\theta),$$

where θ is the angle between the direction the -rays are emitted and the orientation axis. The quantities $B_k(T)$ describes the initial orientation of the nuclei and contains all the temperature dependence of $W(\theta)$. The U_k are angular momentum reorientation parameters, the R_k are angular correlation coefficients, and the $P_k(\cos\theta)$ are the Legendre polynomials.

Only even terms enter in the summation of k because only the directional distribution of the radiation is of interest and not the state of polarization of the γ-rays. The summation over k goes from zero to the lesser of 2L or 2I, where L is the multipolarity of the emitted rediation and I is the spin of the oriented nucleus. For the purposes of this thesis it is sufficient to know that the sum can be calculated to the necessary accuracy.

Consideration of $W(T,\theta)$ shows that the largest temperature variation in radiation flux with changes in the temperature occurs at $\theta = 0^\circ$ or 180°. Furthermore, the relation between temperature and W is unique at these points, whereas at directions where $P_k(\cos\theta)$ is zero, this is not true. The two most commonly used nuclei in NOT are ^{60}Co and ^{54}Mn, for which the decay processes are well understood and the coefficients in equation (27) can be calculated. For ^{60}Co, W(T,0) is given by

$$(28) \qquad \omega(T,0) = 1.1905 + 0.01582 \Sigma m^2 \rho(m) - 0.039682 \Sigma m^4 \rho(m),$$

where $\rho(m)$, the population of the m th sublevel as given by equation (25), is the only temperature dependent quantity. The index m is summed from I to -I, where I is the nuclear spin equal to 5 for ^{60}Co and 3 for ^{54}Mn. Similiarly, for ^{54}Mn one has

(29) $$\omega(T,0) = 1 + 0.38887 \Sigma m^2 \rho(m) - 0.00319 \Sigma m^4 \rho(m) \}$$

The degree of alignment is related to the ratio $\Delta E/kT$, where $\Delta E = u_n g_n B$, the hyperfine splitting.

The radioactive nuclei are oriented by diffusing them into a host material which is magnetic. The internal local field can be of the order of 10 - 30 T in the iron group metals. The domains in the host are aligned by applying a magnetic field of 0.1 - 1 T. Some care must be taken to ensure that the applied field is sufficient to align all the domains.

The NOT is a practical primary thermometer(Krane et al, 1973), because the hyperfine splitting in the host material can be measured with high precesion by NMR experiments. Measured E for ^{54}Mn in iron is $\Delta E/k = 9.11 \pm 0.01$ mK, and for ^{60}Co in iron $\Delta E/k = 7.945 \pm 0.003$ mK(Templeton and Shirley, 1967). The range of temperature over which the NOT can be used as a thermometer is limited because it is sensitive only for temperature approximately $\Delta E/k$. The most commonly used nuclei, ^{60}Co and ^{55}Mn, are almost completely aligned at 30 mK. Recently ^{166}Ho in a single crystal of Ho has been used(Marshak, 1982) to to cover the range 32 mK to 1.2 K, but ΔE has not yet been measured by NMR, therefore it must be considered a secondary thermometer.

The theoretical accuracy of the NOT is limited by the fact that W(T,0) applies to a point source, although in practice most experimental configurations approximate the condition quite

well. Also, W(T,0) applies to a point detector, whereas all detectors have a finite surface area. As long as the detectors are cylindrical, the form of W(T,0) is modified only by an attenuation factor ,Q_K, in the the sum(Rose, 1953).

The technical problem of aligning the source with the detector and measuring the solid angle accurately contributes to the uncertainty in the measured temperature. The demagnetization effects of the host material must also be taken into account when calculating the effective field at a site, even in a thin foil specimen.

The major disadvantage of NOT is the long counting times necessary for accurate measurements of the temperature. The statistical error, Δn, in a measured count is $\Delta n = n^{1/2} = (n_b + n_o W(T,0))^{1/2}$, where n_o is the number of pulses in the high temperature limit and n_b is the background count. To keep the self-heating of the thermometer low, the flux has to be kept small, and this implies relatively long counting intervals. Counting times longer than 30 minutes should be avoided as it becomes too tedious in practice(Lounasmaa). Of the two, the ^{54}Mn thermometer is more accurate than the ^{60}Co thermometer at temperatures less than 20 mK because it self-heats an order of magnitude less than the ^{60}Co. If the γ-ray absorption is ignored(this is very small as long as the cryostat is not too bulky), the radioactive self-heating of 1 uCi of ^{60}Co is 630 pW as opposed to 30 pW for 1 uCi of ^{54}Mn.

The ^{54}Mn self-heats less than ^{60}Co because it decays through electron capture, whereas ^{60}Co decays through emission of 110 Kev electrons.

The most common host material for ^{60}Co and ^{54}Mn is iron(Sites et al, 1971, Johnson et al, 1972), although nickel and cobalt have been used(Cameron et al, 1967). If ^{60}Co is distributed uniformly throughout a hcp ^{59}Co single crystal(Thorp et al, 1970), then no external polarizing magnetic field is necessary. ^{54}Mn will not diffuse into hcp cobalt crystals. A further reason for preferring ^{54}Mn in Fe is that it has a spin-lattice relaxation time of the order of 1 minute at 2 mK, whereas ^{60}Co in Fe has a T_1 of 7 minutes at 2 mK.

In Kondo materials, below the Kondo temperature, the hyperfine field is independent of the temperature and a very strongly dependent upon the applied field. If the hyperfine field is known as a function of the applied field, then the hyperfine splitting can be adjusted to give the maximum sensitivity in the region of interest. Two possible systems which have been studied are ^{54}Mn doped to less than 1 ppm in pure copper(Pratt et al, 1969), and ^{54}Mn doped to less than 1 ppm in zinc(Marsh, 1970). Both themometers have been found to be most sensitive in the range 1-20 mK.

The temperature range of ^{60}Co or ^{54}Mn NOTs is from a few mK to 30 or 40 mK with an accuracy of 1% when using a counting time of a few minutes per point(Sites et al, 1971).

Temperatures below 1 or 2 mK can be measured with a NOT using a Kondo material as the host film and carefully controlling the applied magnetic field. The "brute force technique" of alignment of the nuclear spin with applied filds of the order of several Tesla can be used to extend the NOT down to the microKelvin range(Ono et al,1980)°, where interactions between the nuclei become important. When lower temperatures are measured, it must be remembered that the nuclear spin temperature need not be the same as the lattice.

1.5.10 Thermal Noise Thermometry

Nyquist(1928) formulated a relation between the random voltage generated across a resistor and the Brownian motion of conductive electrons in the resistor using the second law of thermodynamics and the law of equipartition of energy. The most common form of the relation is

$$(30) \qquad \langle v_n^2(t) \rangle = \int 4RkT\,dv \;,$$

where $\langle v^2(t) \rangle$ is the time average of the thermal voltage fluctucations squared, R is the resistance of the element, and the integral is over the frequency range over which the voltage is measured. Nyquist generalized the fluctuations to include quantum mechanical effects, but the most general thermal noise relation includes zero-point fluctuations(Callen and Welton, 1951) and is as follows

$$(31) \qquad \langle V_n^2(t) \rangle = \int_0^\infty 4h\nu R(\nu) \left[\tfrac{1}{2} + \frac{1}{e^{h\nu/kT} - 1} \right] d\nu \;.$$

Furthermore, the resistance R in (30) has been generalized to a frequency dependent resistance. In the limit $h\nu/kT \rightarrow 0$, equation (31) reduces to Nyquist's original equation. The experimentally measured thermal noise has agreed very well with the theoretical predictions, thus in principle thermal noise

thermomtry can be used to define the temperature scale(Johnson, 1928, Soulen and Marshak, 1980).

The difference in temperature found by using (30) instead of (31) is given by

(32) $$\frac{\Delta T}{T} = \left(\frac{h\nu_c}{kT}\right)^2 \frac{1}{36} = 6.4 \times 10^{-23} \left(\frac{\nu_c}{T}\right)^2 K^2 sec^2 .$$

It is calculated by expanding the integrand in equation (31) in powers of $h\nu/kT$, integrating the series, and then evaluating the result using a high frequency cutoff at ν_c. If the cutoff frequency is less than 12.5 MHz and the temperature being measured is more than 1 mK, then accuracies of better than 1% can be achieved by using (30) instead of the more complicated relation (31).

The basic components of a noise thermometer(NT) are a resistor at the temperature of interest, an amplifier, and a power meter. The amount of noise an amplifier adds to a signal can be described quantitatively by a noise temperature. The noise temperature of the best room temperature amplifiers is 10 - 20 K. The noise temperature is added linearly to the noise from the resistor of interest, so that a very large correction must be subtracted from the output of the amplifier if the resistor is at a few mK. Other difficulties in the implementation of the NT is that the frquency response of the amplifier must be well known and the 1/f noise spectrum from

thermal emf's must be carefully accounted for. A description of the many techiques which have been developed to circumvent these problems is given by Kamper(1973).

At low temperatures, the use of Josephson junctions and superconductors permits the measurement of noise power without adding excessive amounts of noise to the signal. There are two ways to exploit the various characteristics of the superconducting device. One method is to use a squid magnetometer to directly measure the noise voltage(Webb et al, 1973). The second method is to apply the noise voltage to a Josephen junction and to use the voltage to frequency conversion property of the junction(Webb et al, 1973). The temperature is inferred from measurements of the frequency: the power output of the system is not measured so the amplifier gain chacarteristic need not be known.

The squid magnetometer NT achieves the very low amplifier noise(0.05 mK) (Webb et al, 1973) by using the squid in the flux locked mode to balance the noise voltage generated in the resistor. The circuit consists of three parts. The temperature sensing resistor, R, is connected to a superconducting inductor, L, which is flux coupled to a Squid. The squid is operated as a null detector and is connected to a feedback system, which maintains a fixed flux in the squid. The current needed to maintain a constant flux in the squid is processed through an active bandpass filter and then an integrating mean square

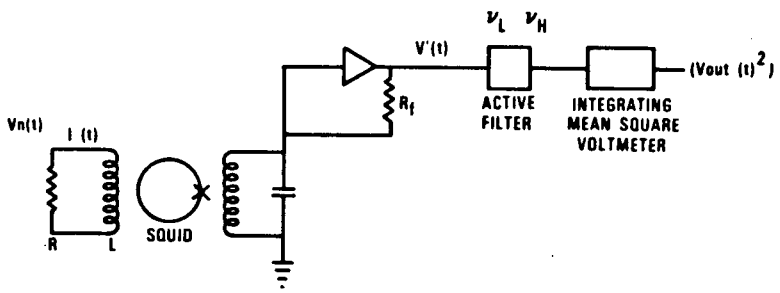

Figure 1. A Squid magnetometer noise thermometer with low noise characteristics as used by Webb et al(1973).

voltmeter. The system operates as follow, the noise voltage, v(t), induces a current, I(t), in the inductor. The squid magnetometer measures a flux $\phi(t) = LI(t)$. The feedback system then passes a current, I'(t), which generates a flux equal to $\phi(t)$, in the squid. The current, I'(t), passes through a resistor, R_f, and the voltage v'(t) is then processed by a bandpass filter and measured in a powermeter.

The noise temperature of the system is found by performing a model calculation on the whole system. By suitably adjusting the parameters, such as, R, L,and r, the noise temperature of the system can be decreased to 0.05 mK. The transfer function of the system must be known accurately before the NT can be used as an absolute thermometer. The absolute accuracy of a squid magnetometer NT is 3%, and is mainly due to uncertainties in L and R.

One alternative is to use the NT as a secondary thermometer by calibrating it at a single fixed point. The components must be carefully compensated or measured to account for changes in the parameter values as the temperature changes.

The quantity of interest $\langle v^2(t) \rangle$ is a statistical quantity since a finite integration time is used. There is a conflict in the choice of parameters. In order to minimize the noise temperature of the system and to minimize the statistical error in a given measurement, a compromise of an averaging time of 2000 - 2500 secs and a precision of 1% for 68 % of the

measurements of the temperatures between a few milliKelvin and 20 K have been used(Webb et al,1973).

The second method ulitilizes the fact that the current in a weak link which has an applied d.c. bias voltage, V, oscillates at a frequency, f, given by

(33) $$hf = 2eV,$$

where e is the electron charge. The Josephson junction is biased with a voltage, U, so that the noise voltage, v(t), modulates a frequency given by equation (33) with U as the voltage. The frequency is usually choosen to be 5KHz. The small amount of power radiated by the junction(of the order of 10^{-15} W). is amplified by parameteric up-conversion. This is accomplished by supplying a 30 MHz carrier signal to the junction. The signal is further amplified and then demodulated by room temperature electronics. One way of interpreting the resultant power spectrum is to realize that the noise voltage fluctuations are compressed(Burgess, 1967) into a Lorentzian curve with FWHM given by

(34) $$\delta f = 4\pi kTR/\phi_o^2.$$

where ϕ_o is the quantum of flux equal to h/2e. The method has been used to test the noise thermometer to 10% in the range 1 -

8 K(Silver et al, 1967).

The temperature can also be inferred from N frequency measurements of the system. The variance, σ, of the N measurements is calculated as

$$\sigma = \sum_{i=1}^{N} \frac{(\nu_i - \nu_{i+1})^2}{2N}, \tag{35}$$

where ν_i is the frequency measurement on the i th trial. The variance can be related to the temperature of the resistor by(Kamper and Zimmerman,1971)

$$\sigma = 2Rk T/\phi_o^2 \tau \tag{36}$$

where τ is the gate time of the frequency counter. By taking a large number of frequency measurements, the variance can be determined to the desired accuracy, thus the second method is more useful than the first. In either case, the equations contain easly measureable quantities and constants; thus the thermometers are good primary thermometers. The resistor of the system can be determined in the same experiment by measuring the current in the resistor and averaging the frequency output of the system to get the voltage by equation (33).

There are two unavoidable sources of uncertainly in the thermometer. The number of frequency measurements that can be made is finite, therefore, there is a statistical error

associated with the calculated variance. Simple calculation show that the rms scatter, ΔT_{RMS}, in the determined temperature is given by

$$\frac{\Delta T_{RMS}}{T} = \left(\frac{2}{N}\right)^{\frac{1}{2}} . \tag{37}$$

There is a count imprecision of 1 in the frequency measurement which adds an extra contribution to the variance. The effect can be considered to be the device noise, T_D, and has been calculated(Kamper and Zimmerman, 1971) to be

$$T_D = \frac{\phi_0^2}{2kR\tau} \tag{38}$$

When the systematic correction in the measured temperature is equal to the uncertainty in the measurement, then the adjustment of the measured temperature is not useful. This sets a limit on the resolution T of the thermometer. Combining (37) and (38), one finds that the minimum resolution of a NOT is

$$\frac{\Delta T}{T} = \frac{3.65 \times 10^{-8} \Omega \text{ sec}}{R \tau N^{1/2}} . \tag{39}$$

To obtain a uncertaintly of 1% in the measured T, the number of frequency measurements required is 2×10^4. If the averaging time is 1 sec then the total time necssary to measure

the temperature at one point is 6 hours.

The unavoidable systematic errors have beeen predicted to be in the microkelvin range(Stephen, 1969).

In summary, the noise thermometer is the primary thermometer the least troubled by corrections to the measured temperature. It is capable of measuring temperatures from a few mK to 0.5 K with 1% uncertainty. A major disadvantage of the NT is that it requires nearly an hour to measure a single temperature accurately. Also, there always exists the possibility of an undetected extraneous noise source in the system which is undetected.

II. ^{3}He Melting Curve

2.1 Introduction

The ^{3}He melting curve and the melting curve thermometer(MCT) characteristics will now be discussed in some detail, in order to substantiate claims made earlier. Although both liquid and solid ^{3}He are quantum systems, the thermodynamic Clausius-Clapeyron equation

$$\frac{dP_m}{dT} = \frac{S_l - S_s}{v_l - v_s} \quad ; \tag{40}$$

describes the melting curve. If all the terms on the right hand side of (40) were known, then the melting curve could be constructed by integrating equation (40). The usual procedure(Scribner et al, 1969), is to accurately measure $v_l - v_s$ and use the values in equation(40). Then the shape of the melting curve is determined by the molar entropy of the liquid and solid ^{3}He. At pressures less than 40 bar and high temperatures, the P-T diagram of ^{3}He is not particularly interesting, but at low temperatures there are several phase transitions (Halperin et al, 1978). Along the melting curve, there are three triple points which correspond to the A-transition in liquid ^{3}He, the B-transtion in the liquid, and

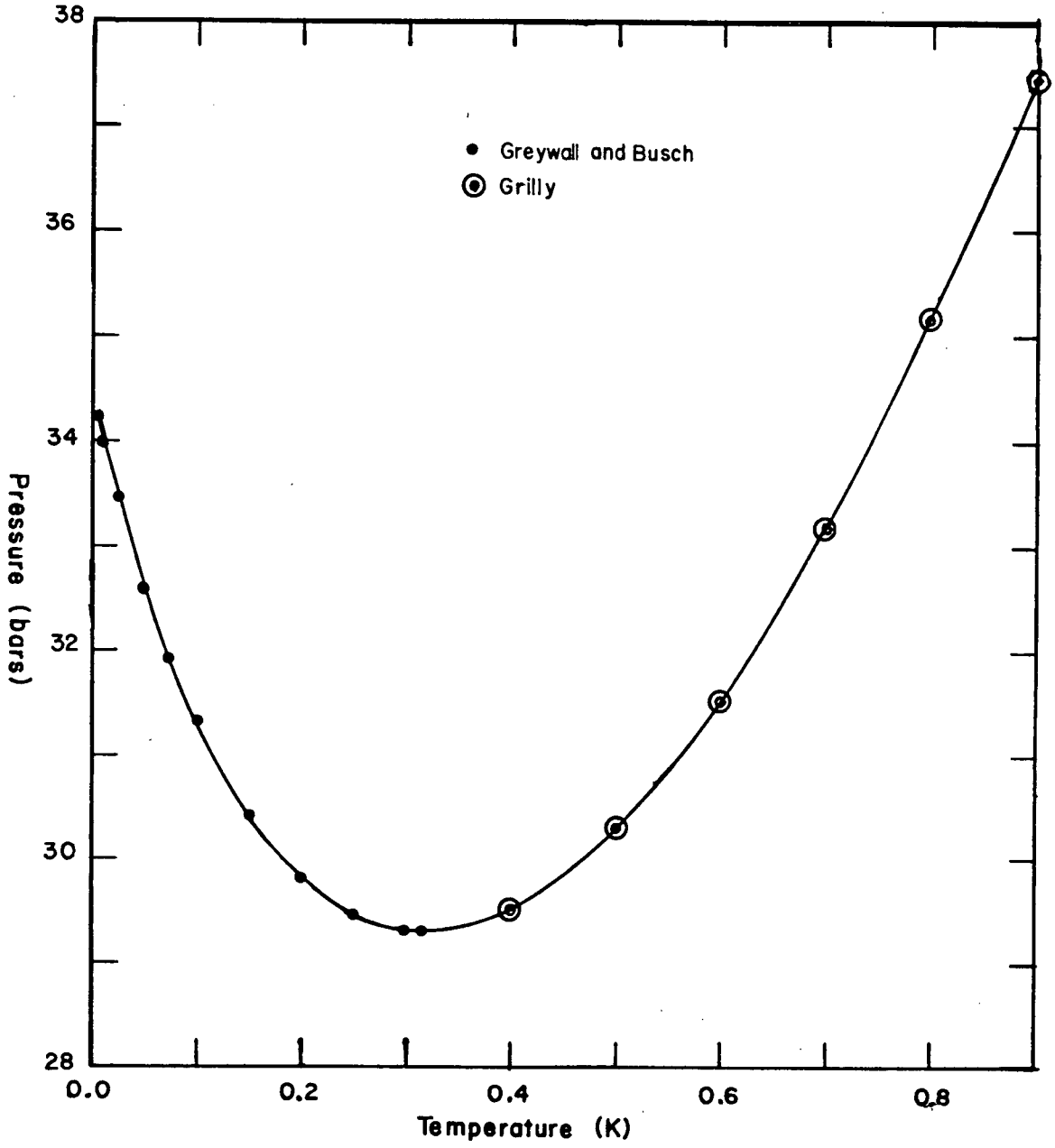

Figure 2. The melting curve of ^3He using the results from Greywall and Busch (1982a) and Grilly(1971)

the magnetic transition in solid ^{3}He. Although very interesting and useful as thermometric fixed points at very low temperatures(Roger et al,1983), they will not be considered in the context of this thesis, since they occur below the base temperature of the refrigerators in this lab.

There are no accurate theories for the entropy of the various phases of ^{3}He along the melting curve. The ^{3}He liquid behaves like a Fermi-liquid down to the A-transition (Legget, 1975), thus its entropy should be a linear function of the temperature (Wilks). Experiments suggest, however, that there are higher order terms in the expression for the entropy of the liquid (Abel et al, 1960). The liquid commences to spin order at about 0.5 K(Scribner, 1969), so that its entropy is very small at the millikelvin temperatures. Theoretically, the entropy is expected to be unaffected by magnetic fields which can be experimentally applied(Goldstein).

The semi-classical model of solid ^{3}He is that of a system of non-interacting spin 1/2 particles sitting at equilibrium sites. The system has a molar entropy of Rln2(Kittel). The lattice entroy contributions are very small as the Debye temperature of solid bcc ^{3}He is 20 K(Halperin). The entropy of the solid would be expected to decreases as the spins begin to order due to the nuclear dipole-dipole interactions, which have a characteristic energy of 10^{-7} K. Above 50 mK, the measured spin entropy is as predicted (Halperin et al), but near 1 mK the

entropy suddenly decreases to 0.1Rln2 (Osheroff, 1972). The spin ordering in the solid occurs at a higher temperature than expected because the zero point motion of the ^{3}He, which is aproximately 30% of the nearest neighbour separation, results in large exchange overlap interactions, of the order of 1 mK. If only nearest neighbour exchange is taken into account, the spin Hamiltonian of the system has the same form as the Heisenberg form(Thouless,1965)

$$H_{ex} = -2 \sum_{i<j} J_{ij} I_i I_j \,, \tag{41}$$

where J_{ij} is the exchange interaction between two neighouring atoms i and j, and I is the nuclear spin operator. Solid ^{3}He is anti-ferromagnetic, so the coupling constants J_{ij}'s must be negative. High temperature series expansion of the partition have been found for solid ^{3}He by Goldstein(1967). At the low temperatures the qualitative behaviour of the solid is not described by the Heisenberg model. The model predicts a second order transition at about 2 mk, but experiments have shown a first order transition at about 1 mk. It predicts a decrease in the susceptibility relative to the Curie-Weiss law, but experiments(Bernier and Delrieu, 1977), shows that the susceptibility increases. A complete list of the defficiency of the Heisenberg model is given by Roger et al (1983). The latest model suggested to explain the behaviour of solid ^{3}He below 30

mK is that of a system of atoms which have multiple exchange interactions(Roger et al). Although the very low temperature behaviour of the melting curve is difficult to explain theoretically, the higher temperature characteristics are quite well understood.

The shape of ^{3}He melting curve about the minimum can be explained by a relatively simple model. The entropy of the solid, in the range 10 mK to 500 mK, is Rln2, because the ^{3}He particles are non-interacting spin 1/2. The entropy is temperature independent until 10 mK, where due to ordering of the spins it decreases rapidly. The liquid ^{3}He is a degenerate Fermi gas whose entropy decreses rapidly below 0.3 K and is equal to the solid entropy at 0.32 K. The molar volume difference between the solid and the liquid is approximately constant(Scribner et al., 1969) from 0.33 K to zero K. At T = 0.32 K where the two entropies are equal, the Clausius-Clapeyron implies that the melting curve has an extrema. After inserting the quantities into equation(40) and integrating it, one finds a curve similiar to the measured curve. More sophisticated models have tried to predict the entire melting curve but no accurate melting curves have been generated(Hudson et al.).

Given that it is not certain that even the newer theories accurately describe the behviour of the ^{3}He along the melting curve, an empricial approach will be used to justify the claims made about the ^{3}He melting curve thermometer.

Because there is no complete theory for the ^{3}He melting curve, the MCT is calibrated by comparing the melting cruve with a primary thermometer. The most recent and precise measurement of the ^{3}He melting curve is by Greywall and Busch(1982a), who used the temperature scale set by NBS through the SRM 768 fixed point devices. They found the minimum pressure to be 29.316 0.003 bar. at a temperature of 0.318 0.001 K. Their results agreed with accurate measurements made by Halperin et al at the very low temperatures, and with the results of Grilly at the minimum in the curve. Greywall and Busch fitted the function below to their data.

$$P - P_A = \sum_{i=-2}^{5} a_i T^i , \qquad (42)$$

where P_A = 32.342 bar and T_A = 2.752 mK, the A-transtion coordinates found by Halperin et al. The coefficients are

$a_{-2} = 8.406 \times 10^{-8}$	$a_{-1} = -1.220 \times 10^{-4}$
$a_0 = 0.15435$	$a_1 = -44.4713$
$a_2 = 157.616$	$a_3 = -365.784$
$a_4 = 624.330$	$a_5 = -491.348$.

The data of Greywall and Busch, and Halperin et al, deviates

from the values given by the expression (42) by less than 2 mbar, which corresponds to 0.5% uncertainty in the measured temperature over most of the temperature range of the thermometer.

2.2 Magnetic Field Dependence of the Melting Curve

The slope of the ^{3}He melting curve is proportional to the difference $s - s$, and since the entropy of a Fermi liquid is only slightly affected by the magnetic field(Goldstein, 1968), the slope of the curve is proportional to the entropy of the solid ^{3}He. In the Heisenberg approximation of the ^{3}He solid, the entropy is given by (Goldstein, 1967)

$$(42) \qquad \frac{S_s}{R} = \ln 2 - \frac{3x^2}{2} + x^3 + \cdots, -\frac{1}{2}y\left[1 + 8x + 36x^2 + \cdots\right] + \cdots,$$

where $x = J/kT$ and $y = Bu/kT$. B is the magnetic field, and u is the magnetic dipole moment of the ^{3}He atom. The J is the Heisenberg coupling constant between nearest neighbours in a ^{3}He solid and is of the order of -1 mK(Trickey, 1972). In all experimental conditions y is very small, but even if $y \to 1$, as long as the model is considered in the region $T > 1$ mK, where $x < 1$, the entropy is essentially independent of the interaction characteristics, because the coefficient of y^2 in (42) contains x as a second order term. Although at temperatures below 40 mK(Scribner) and high magnetic fields, the Heisenberg model is incapable of describing the melting curve, as even its quantitative predictions are incorrect, the Heisenberg model can be used above this temperature to describe the melting curve respond to a applied magnetic field. At the very low

temperatures, the multi-exchange interactions must be included in the model to get satisfactory agreement with the observed behaviour.

It has been experimentally found(Kummer et al., 1977) that for temperatures greater than 1.35 mK and magnetic fields less than 4.5 KG the depression of the melting pressure is unresolvably small. Even for fields as high as 12 kG, as long as the temperature is above 10 mK, the measured temperature will be accurate to better than 1 % of the reading(Hummer et al., 1977). The melting curve has been measured in magnetic fields as high as 63 kG(Johnson et al, 1971), but thermometry problems prevented the useful interpretation of the data.

That the melting pressure is depressed in the presence of a magnetic field can be shown thermodynamically by considering the Gibb's free energy of two magnetized phases in equilibrium. It is easy to show that at a constant temperature

$$\frac{dP_m}{dT} = \frac{M_\ell - M_s}{V_\ell - V_s} \tag{43}$$

where M_ℓ and M_s are the molar magnetization of the liquid and the solid. Neglecting the magnetization of the Fremi liquid because it is small(Goldstein, 1968), one gets

$$\frac{dP_m}{dT} \simeq \frac{-M_s}{V_\ell - V_s} = \frac{-M_s}{\Delta V}, \tag{44}$$

where v is approximately constant and greater than zero. As the magnetic field is increased, the magnetization increases and the melting pressure is depressed.

2.3 Impurity Effects on the Melting Curve

The melting curve minimum occurs at higher temperature and at a depressed pressure as the ^{4}He concentration in ^{3}He is increased (Weinstock et al., 1962). No major study has been made of the effect of increased ^{4}He concentrations on the curve, but Scribner et al.(1969) found no substantial difference between the melting curve with 20 ppm ^{4}He and 600 ppm. But a small bump at a temperature of 0.1 K was noticed in the melting curve with 600 ppm ^{4}He. So as long the ^{4}He concentration is smaller than 20 ppm then the bump should be unresolvably small, the phase separation that occurs in the ^{4}He ^{3}He mixture probably insures that the ^{3}He is very pure at the low temperatures. Furthermore, the ^{4}He will tend to solidify on the sinter in the ^{3}He cell. An estimate of the amount of ^{4}He which can be frozen out onto a surface is found by estimating the area per atom and dividing into the total surface area available. The nearest neighbour separation in bcc solid helium at 29 bars is about 4 A(Keller). The atom diameter is 2.2 A. The surface area of the sinter in a cell of the Greywall and Busch type is 0.5 m^2. The total amount of ^{3}He is the cell and capillary below the plug is about 4×10^{-4} moles, thus, assuming that the spacing per atom in a monlayer is approximately equal to the lattice separation in three dimensions, the ^{4}He concentration can be as high as 700 ppm and it will still freeze out onto the sinter surface in a monolayer.

A monolayer of ^{4}He will not affect the Kapitza resistance of the sinter(Harrison). Most ^{3}He melting curve thermometers have used ^{3}He with ^{4}He impurities less than 20 ppm(Greywall and Busch, 1982a).

2.4 Accuracy and Resolution of the MCT

The resolution of the MCT depends on the resolution of the strain gauge used to measure the pressure at melting. Most pressure transducers used for thermometry(Greywall and Busch, 1982a, Corrucini et al, 1978) have a pressure resolution of better than .1 ppm. The temperature sensitivitly of the melting curve increases as the temperature decreases down to about 3 mK where the curve beginning to level off as required by the third law of thermodynamics. This leveling off can be seem in the values of the $\frac{dP}{dT}$ listed in Table I, which are the results given by Greywall and Busch(1982a). At T = 300 mK, the temperature resolution, given $\Delta p/p = 10^{-7}$, is 3 μK, and the resolution increases at the lower temperatures. If a good dead weight tester is used to calibrate the strain gauge, then the pressure measured by the strain gauge will have a uncertainty in the accuracy of 0.003 bar(Greywall and Busch, 1982a) or better (Grilly,1971). At T = 300 mK, 3 mbars corresponds to 3 mK uncertainty, at T = 200 mK, this corresponds to 0.3 mK uncertainty, and finally at T = 100 mK, 3 mbars corresponds to 0.1 mK uncertainty in the measured temperature. Thus the accuracy of the MCT in the range 3 mK < T < 300 mK is better than 1 %, if the pressure is measured to an accuracy of 3 mbar.

The accuracy of any MCT depends on the accuracy to which the ^{3}He melting curve is known to. Greywall and Busch(1982a)

TABLE I

T, mK	P, bar	dP/dT, bar K^{-1}	T, mK	P, bar	dP/dT, bar K^{-1}
3	34.3330	−36.21	90	31.5407	−23.32
4	34.2957	−38.23	95	31.4262	−22.47
5	34.2569	−39.39	100	31.3159	−21.66
6	34.2171	−40.01	110	31.1072	−20.10
7	34.1769	−40.32	120	30.9136	−18.63
8	34.1365	−40.44	130	30.7343	−17.24
9	34.0961	−40.45	140	30.5685	−15.93
10	34.0557	−40.37	150	30.4154	−14.69
11	34.0154	−40.25	160	30.2745	−13.50
12	33.9752	−40.09	170	30.1452	−12.37
14	33.8954	−39.71	180	30.0268	−11.30
16	33.8164	−39.26	190	29.9191	−10.26
18	33.7383	−38.79	200	29.8215	−9.27
20	33.6613	−38.30	210	29.7336	−8.31
25	33.4729	−37.05	220	29.6551	−7.39
30	33.2907	−35.81	230	29.5856	−6.51
35	33.1147	−34.58	240	29.5248	−5.65
40	32.9448	−33.39	250	29.4725	−4.82
45	32.7808	−32.23	260	29.4282	−4.03
50	32.6224	−31.11	270	29.3918	−3.26
55	32.4696	−30.02	280	29.3630	−2.52
60	32.3222	−28.97	290	29.3414	−1.81
65	32.1799	−27.95	300	29.3267	−1.14
70	32.0426	−26.96	310	29.3185	−0.50
75	31.9102	−26.00	320	29.3166	0.10
80	31.7826	−25.08	330	29.3204	0.66
85	31.6594	−24.18			

Table of various parameters of the melting curve as calculated by Greywall and Busch (1982a).

measured the melting curve to accuracies of 3 mbar in the pressure and a few tenths of a percent in the temperature.

2.5 Self-heating and R.F. Sensitivity of the MCT

The self-heating of a MCT originates from the joule heating in the coaxial cables which are connected to the capacitor of the MCT pressure transducer. The amplitude of the a.c. excitation voltage must be kept to a minimum to reduce the joule heating in the wires, but this limits the measurable resolution of the capacitor. An excitation voltage of 2 volts RMS means that during the nulling operation, voltages on the order of microvolts must be measured if the capacitance of the transducer is to be measured to 1 ppm. A lock-in detection system must be used to measure the voltages because thermal emfs and stray electrical noise would otherwise obscure the signal. The requirement that the capacitance be resolvable to 1 ppm sets a lower limit on the usable excitation voltage. If the excitation voltage in 2 volts RMS, then with careful thermal grounding of the cables, the power dissipation in the MCT can be less than 10^{-14} watts.

The MCT is insensitive to r.f. noise because the large impedance of the capacitor in the transducer allows only a very small current to flow in the lead wires, thus there is very little joule heating.

2.6 Thermal Time Response of the MCT

The thermal response time, τ, of the thermometer attached to a thermal bath is determined by the heat capacity of the thermometer, C_{ef}, and the resistance, R, to the heat flow to bath by

$$\tau = RC_{ef}. \tag{45}$$

There are really two thermal systems that need to be considered for a precise determination of the thermal response time. The first system consists of the BeCu strain gauge. The specific heat of the BeCu is about an order of magnitude smaller than that of ^{3}He liquid(Lounasmaa) and the conductivity of the BeCu is approximately the same order of magnitude as the ^{3}He liquid. Because the cell is in metallic contact with the heat bath, the thermal boundary resistance is much smaller than the Kapitza resistance between the liquid ^{3}He in the cell and the walls of the cell. The second system consists of the solid and liquid ^{3}He and the walls of the cell. The thermal conductivity of the liquid ^{3}He is fairly large at the low temperatures being considered(Lounasmaa), therefore as long as there is liquid in the cell, the ^{3}He phases are in equilibrium. This is not strictly true at the very low temperatures(Scribner et al., 1972), but the approximation will suffice for these

calculations. The thermal time constant of the ^3He is a good estimate of the thermal time constant of the thermometer. By considering the melting process as heat is introduced into the ^3He system, and using representative low temperature values for the ^3He parameters (Corrucinni et al, 1978), one gets that the effective heat capacity, for $T < 100$ mK, is at most $5.6 \times 10^8 nT$ erg/(mole K^2), where n is the number of moles of ^3He. The measured Kapitza resistance between ^3He and silver sinter is $R = 0.24 T^{-3} A^{-1} K^4 m^2/Watts$, for $T > 10$ mK(Godfrin), where A is the effective surface area of the sinter in square meters. Thus equation (45) gives the thermal time to be

$$(46) \qquad \tau = \frac{13.4\, n}{A T^2} \ m^2 K^2 \text{ sec} \ .$$

The surface ares of 700 A silver sinter in a melting curve thermometer of the Greywall and Busch(1982a) type is 0.5 m^2. The thermometer cell contains 0.09 cm^3 ^3He at 34 bars. Thus for $T = 0.05$ K, is at most 40 secs. If the temperature of the cell is below 10 mK, then the Kapitza resistance of the silver sinter is given by(Harrison, 1979)

$$(47) \qquad R = \frac{1.10 \times 10^{-4}}{AT} \ m^2 K \frac{\text{sec}}{\text{erg}} \ ,$$

thus $\tau = 450$ secs. So below 10 mK, the thermal time constant of the thermometer is at most 7 minutes. Fortunately, for the

operating conditions of the cell, the thermal time constant is about 30 sec. (Greywall and Busch, 1982a).

III. ^{3}He Melting Curve Thermometer

3.1 Introduction

The ^{3}He melting curve thermometer consists of three parts, a pressure transducer cell with a fixed volume, a capacitance bridge circuit to measure the transducer response, and a pressure system to supply ^{3}He at 35 bars and calibrate the strain gauge.

The pressure transducer cell used at low tempertures must satisfy several requirements; it must be able to withstand repeated cycling to low temperature without developing a leak; it must have a low specific heat so that its thermal time constant is short; it must not be too bulky so that it can be easily fitted onto a dilution refrigerator; and furthermore, the volume of the cell must remain a constant, regardless of the pressure in the cell. Because the strain gauge of Greywall and Busch(1982a) satisfy all these requirements, it as chosen as the capacitance pressure transducer to be used in for this MCT. The required sensitivity in the pressure measurements demands that the capacitance of the transducer be measured to 1 ppm, with a drift over a day of less than 1 ppm. Because the capacitance of the transducer is approximately 10 pF and the capacitance to ground of the coaxial cables is 300 pF, the guarded ground

3-wire technique must be used so that the stray capacitance does not completely mask the response of the transducer. Fortunately, as the measurement of capacitance is a refined technique, the required resolution and stability can be achieved with mostly readily available commerical instruments.

The pressure system of a MCT has many constraints, which makes it difficult to construct. The system must be ^{3}He leak tight over a period of years so that no ^{3}He is lost, and no ^{4}He leaks into the system. Also, the requirement that the volume of the system be small so that only a small quantity of highly purified ^{3}He is necessary to pressurize the whole system to 35 bars, necessitates the use of very thin capillary tubing. The thin capillaries increases the time needed to pump down the system and thus hampers the leak testing of the system. Finally, the ^{3}He must be pressured to 35 bars without contaminating it. These requirements forced many design decisions which makes the pressure system an awkward system to operate.

3.2 Pressure Transducer Cell

The cylindrical pressure transducer of Greywall and Busch (1982a) is shown in Figure 3. It was constructed from 1/2 hardened beryllium copper, type Berylco 25. The parts were hardened after machining by baking at 300 C for 2 hours in a He atmosphere with 0.5 % to 1 % H_2. The treated BeCu has a tensile strength of 585 MPa, and an Young's modulus of 125×10^9 Pa. The thermometer base was made of OFHC copper. Unlike many capacitance gauges of the Straty-Adams type(1969), this gauge does not have any flanges, and consequently, the spacing between the two capacitance plates cannot be adjusted. That feature makes this gauge less bulky and simpler to machine than the other designs, but the assembly of the gauge is correspondingly more difficult.

The first step in the assembly of the gauge was to silver solder a stainless steel 0.56 mm O.D. fill line capillary with 0.13 mm thick walls to the copper base of the thermometer. The bottom of the well in the base was then silver plated so that the silver sinter would adhere to the copper base and form a metallic contact between the sinter and the base. The sintering process will be considered later. About 0.3 grams of sinter was packed into the well; this corresponds to a surface area of 0.8 m^2. The sinter occupies about 45% of the volume of the cell. Next, the diaphragm was epoxied to the base using Emerson

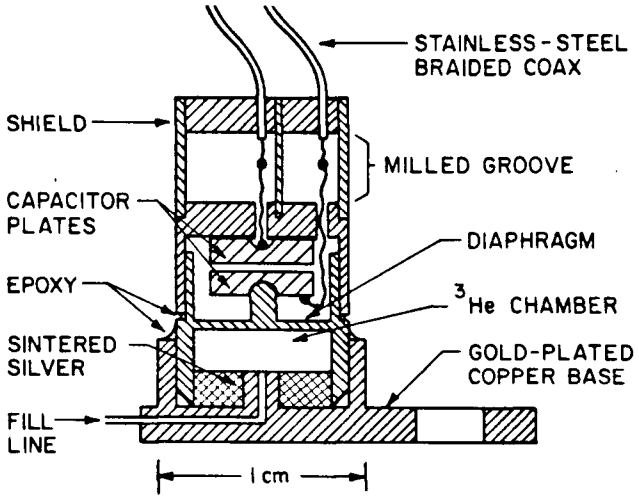

Figure 3. The ^{3}He Strain Gauge used by Greywall and Busch to measure the ^{3}He melting curve.

and Cumming, Type 1266, epoxy. Because the epoxy has a very low visocity, the two pieces were clamped tightly together in a vice to prevent the epoxy from flowing into the sinter. The epoxy was cured for a day under a lamp, before the whole assembly was He leak tested and then pressure tested to 40 bars with He from a high pressure cylinder. Further, the cell was cooled to liquid nitrogen temperature and pressured tested to test that thermal contractions did not crack the epoxy seal.

The diaphragm has a diameter of 0.640 cm and is 0.025 cm thick. Using the formulas given by Straty and Adams(1969), the optimum thickness of the diaphragm for maximum pressure sensitivity is determined by the tensile strength of the BeCu and the pressures that are to be measured.

The capacitor plates surfaces were machined to a fine finish, sanded with very fine emery paper, and then lapped with 10 μm diamond powder for a flat finish. Using inidium solder, #32 brass leads were attached to the plates. The solder flux was completely removed by washing with methanol. An insulating layer of Type 2850 FT epoxy was cured onto the back sides of the capacitor plates. Then the upper plate was epoxied to the housing with 2850 FT and allowed to cure. A drop of 2850 FT was placed on the nipple of the diaphragm, and the lower plate was rested on it. The housing was slipped onto the diaphragm, epoxied with 1266 epoxy, and allowed to rest on the lower plate. The ^{3}He chamber was then pressurized to 34 bar and the whole

assembly cured for 2 days under a lamp. It was found that two days are required for the black epoxy to set, when under pressure and in a small confined volume.

A Boonton Type 74C-S8 capacitance bridge was attached to the leads and the pressure response of the transducer was measured. When the gauge was cooled to LN_2 temperature a large decrease in the pressure sensitivity was measured. Some effort was made to take this shift into account, by decreasing the pressure in the ^3He chamber while the epoxy was curing, but after several trials it was found that the low temperature behaviour was not very predicable. So, the epoxy was allowed to cure at 34 bars pressure which insured there would be no short between the plates within the working pressure range of the MCT. The zero pressure capacitance of 3.15 pF at room temperature implies a plate separation of 3.7×10^{-3} cm. The OFHC copper base was gold plated to ensure good metallic contact when the thermometer is mounted on the mixing chamber of the dilution refrigerator.

3.3 Sinters

Sinters are used in low temperature apparatuses to decrease the Kapitza resistance between liquid helium and the walls of its container. A summary of measured Kapitza resistances for various materials is given by Harrison(1979). Although copper sinters have been used(Lounasmaa), silver sinter is prefered at the lower temperatures because its specific heat is two times smaller than that of copper at 0.020 K(Lounasmaa).

The silver powder commonly used to form the sinter is called ultrafine Ag powder 700 A, Type II and was obtained from the following company:

Vacuum Metallurgical Comp. LTD.
Shonan Bldg. n 14-10
1-Chome, Ginza,
Chuo-ky, Tokyo.

The virgin powder has a surface ares of 4.0 m^2/g as measured by the BET method(Allen,1968) using Ar at LN_2 temperature and using $\sigma = .16\ nm^2$ as the area covered by one Ar atom. A 400 A silver powder is also available from the same company, but because the silver powder tends to self-sinter(Roberston et al., 1983), it is not clear that anything is gained by using the smaller powder, unless very low temperatures will be encountered. The Kapitza resistance of the 400 A sinter is about one half of the

resistance of the 700 A sinter(Godfrin).

The silver is prepared for sintering by first presintering the powder. The oxides are removed from the surfaces of the powder by baking the powder at 380 °C for 10 minutes, while it is flushed with 1-2 torr of hydrogen. After baking it is allowed to cool in a helium atmosphere. The surface to receive the silver sinter must be plated with a thick layer of silver. The silverplate is polished with a fine diamond dust to remove any loose flakes. Then the silver powder is packed onto the surface. In order for the sinter to be structurally strong, the powder must be packed with pressures around 4000 psi. The moderately high packing pressure not only results in a strong sinter, but also increases the surface area of the sinter per unit area of the sinter base.

The sintering is done in a good vacuum or a helium atmosphere; hydrogen should be avoided as it embrittles the copper base of the sinter container. The sinter must must be under pressure during heating because of shrinkage of the sinter. If no pressure is applied, the resulting sinter will be flakey. Greywall claims that 700 A powder packed to 3600 psi pressure and sintered at a temperature of 200 °C for 10 minutes will result in a sinter with a surface area of 2.5 m^2/g.

The sintering parameters are not very critical. Sintering temperatures can be anywhere from 100 °C to 400 °C and sintering times can be from 1 minute to 15 minutes. There is a loss of

surface area of the sintered powder if the higher temperatures or longer times are used, but presumably the sinter will be mechanically stronger. Silver sinter, unlike copper sinter, cannot be machined because it tends to chip off along the pressing layers. The sinter is built up by pressing thin layers of sinter on top of one another, in order to obtain even packing. Otherwise, the sintered powder is very fragile.

The sinter in the MCT cell was made by packing the sinter with a vise and then baking at 90 °C for 20 minutes. With this choice of sintering parameters the sinter was found to adhere well to the base.

3.4 Pressure System

The pressure system for a MCT must be able to pressurize the ^{3}He gas up to 35 bars without contaminating the gas and be able to calibrate the ^{3}He strain gauge with high accuracy. To minimize the contamination, all parts of the system are made of stainless steel and all connections are metal to metal seals. Furthermore, an oil-less compressor was designed to prevent any possibility of pump oil in the system. The pressure system consists of three parts, the charcoal pump, the valves and cold trap network, and the calibration gauge. The arrangement is shown in Figure 4.

The charcoal pump compresses the ^{3}He by absorbing the helium-3 when the charcoal is cooled to 4 K and desorbing the gas when it is allowed to warm up to 30 K. As long as the partial pressure of the helium is greater than 10^{-6} torr, the quantity of helium gas that charcoal at 4 K will absorb is independent of the presssure. The charcoal used in the pump has density of 0.67 g/cm^3 and is able to absorb 0.43 liters STP of helium per gram when cooled to 4 K. Five grams of charcoal were packed into a 17 cm length of 3/8" O.D. stainless steel tube with 0.020" wall, which had end caps welded on. A fill line of 1.22 mm O.D. and 0.20 mm wall stainless steel was welded to one of the end caps. A small filter with pyrex glass wool prevents charcoal dust from entering the fill line. The other end of the

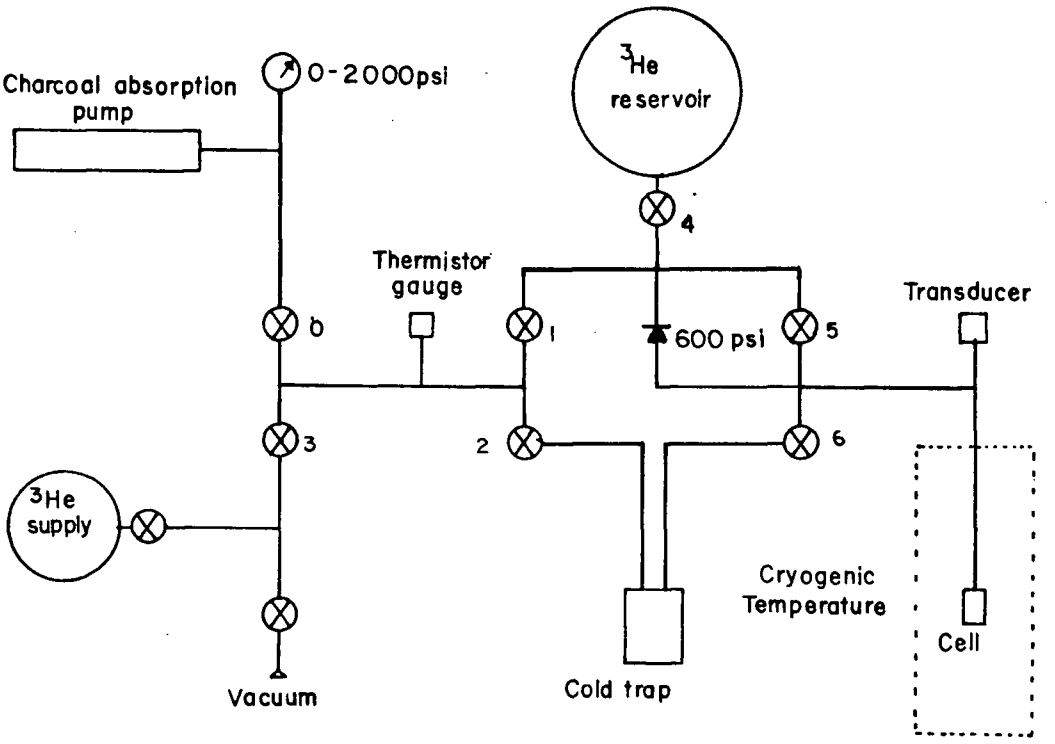

Figure 4. The pressure system for the MCT uses a charcoal pump to compress the ^{3}He to 35 bars. All the valves are bellows valves manufactured by Nupro. Valves 1, 2, 3, and 4 are SS-4BG valves. Valves 5 and 6 are SS-4BRG valves. Valve 0 is a SS-4UG valve. The valve to the vacuum is a brass bellows valve.

fill line is connected to a 0-2000 psi pressure gauge and a Nupro SS-4UG valve. The assembly between the valve and pump will operate safety with pressures up to 140 bars.

A flow cryostat was chosen to cool the sorption pump since there was insufficient space for a helium dewar near the refrigerator. The flow cryostat, shown in Fig. 5, cools by flowing liquid helium over the pump. The pump temperature is monitored with a carbon resistor mounted on the pump; it has a room temperature resistance of 10 kΩ and a liquid helium resistance of 1140 kΩ.

The pump is designed to be used in the following manner: after the pump has absorbed all the helium from the reservoir, it is slowly warmed up with the valve V_o open. When the whole system has pressurized to 25 bars, the valve is closed. The pressure in system is now adjusted by cracking open the valve on the pump.

The network of valves and capillaries are arranged so that the helium can be filtered with a liquid nitrogen trap before it flows into the small capillary tubes. Also, in the event of the dilution refrigerator unexpectedly warming up, a relief valve set at 600 psi opens up to the reservoir. All valves used in the system are stainless steel bellow valves with 1/4" swagelok connectors. The network is designed to operate with pressures less than 40 bars (140 bars for the sorption pump).

When the MCT is not in use, the helium is stored in a

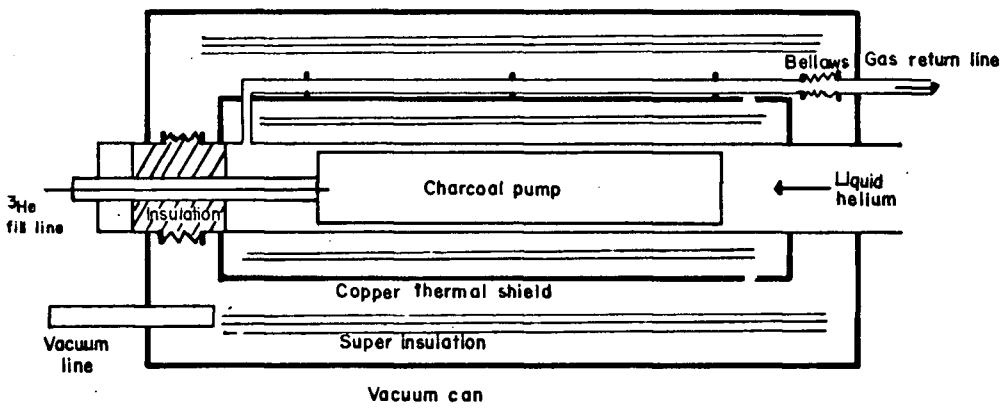

Figure 5. Liquid helium from a storage dewar is forced to flow over the charcoal pump and cool the contents in it.

2570 cc volume at one bar pressure.

The LN_2 cold trap is an 18 cm length of 1/8" O.D., 0.020" wall stainless steel tube filled with crushed 14 A molecular sieve. Although there should not be any large amounts of impurities in the ^3He, the trap helps to ensure that no plugs of foreign gases will be formed in the narrow capillaries which lead into the refrigerator.

The fill line into the cryostat is a capillary with a 1.22 mm O.D. and 0.20 mm wall. At the top of the cryostat the line is silver soldered to a 0.71 mm O.D. and 0.15 mm wall capillary, which continues down to the vacuum can of the dilution refrigerator. There the line becomes a 0.56 mm O.D. and 0.13 mm wall capillary tube. The thin capillary tube is used to decrease the amount of ^3He required to pressurize the system, and ensure that the solid ^3He plug in the tube is fixed to a given point along the tube. Although it requires several days to pump down the system to a pressure less than 10 mT, the impedance of the system is small enough so that the time constant for flow when the pressure is of the order of 10 bars is a few seconds.

A Sensotec Super TJE, 0-600 psi absolute pressure transducer with 0.05% accuracy, repeatibility, and drift is used to calibrate the ^3He cell. It is connected to the pressure network right after the last valve in the system leading to the cell. The power supply for the transducer is a 10.000 volts

supply with a drift of less than 10 ppm. The output of transducer is a 0-30 mV signal, which must be measured with a DVM with an input impedance of not less than $10^{10}\,\Omega$. The sensor was calibrated with a dead weight tester by the manufacture. A least square fit of a quadratic to the calibration supplied by the manufacture gives

$$P = 0.1076 + 1.36480\,v + 2.87698\times10^{-4}\,v^2, \tag{48}$$

where the pressure is in bars and the transducer reading in millivolts. When using the gauge, the zero pressure reading of the transducer must be subtracted from the voltage measurements to get the true voltage output.

The thermistor gauge measures the pressure, by measuring the conductivity of the gas. A rather simple device to construct, its circuit diagram is shown in Figure 6. The gauge was calibrated against a thermocouple gauge using air as the gas. The calibration graph is shown in Figure 7. The gauge was designed because no commerical gauge could be found which can measure microbars and also withstand overpressuring to 35 bars.

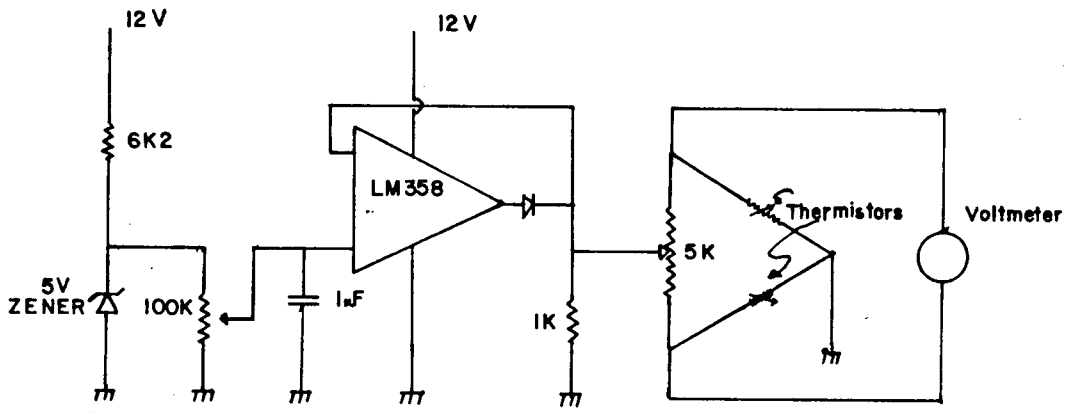

Figure 6. One of the thermistors is exposed to the gas whose pressure is to be measured. The second thermistor compensates for the ambient temperature.

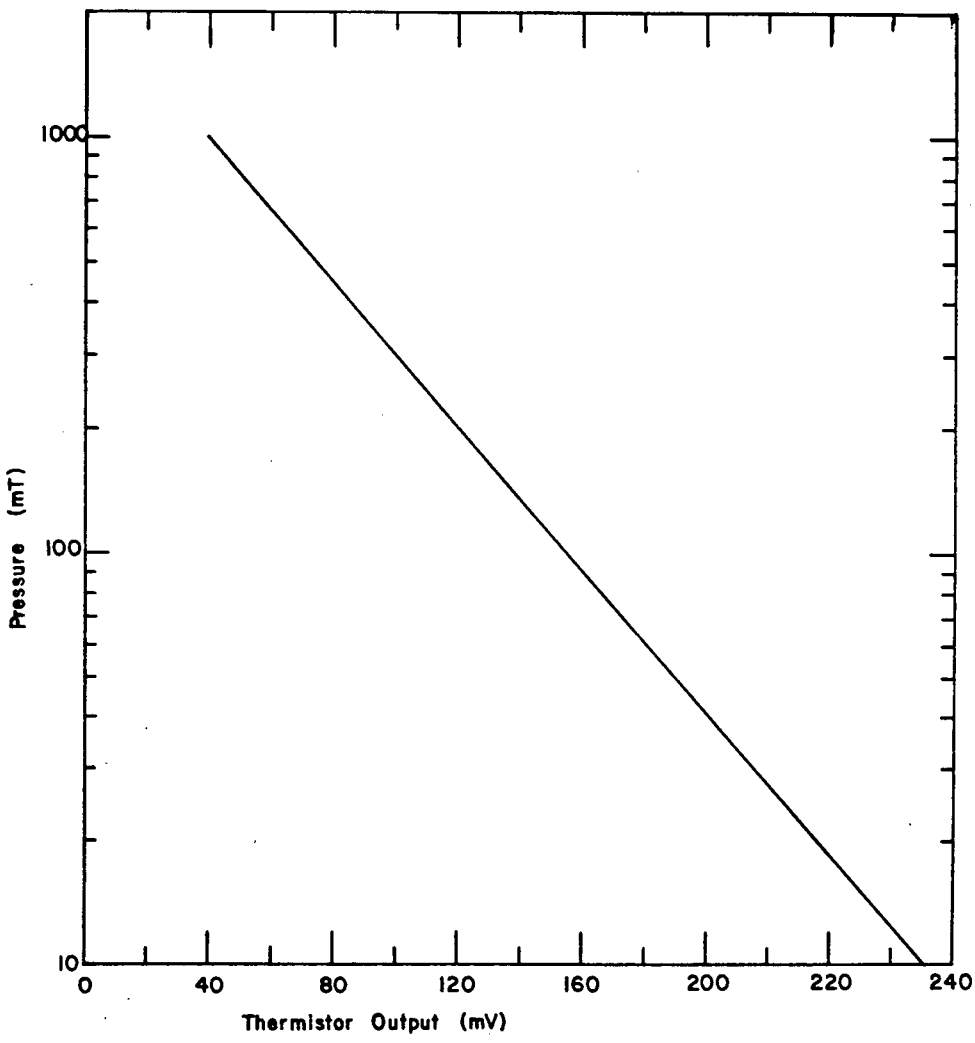

Figure 7. The Thermistor gauge was calibrated against a Thermocouple gauge using air as the gas.

3.5 Capacitance Bridge

A capacitance bridge capable of measuring 10 pF with a resolution of 10^{-5} pF with a short term drift of less than 10^{-5} pF per day is described. The lead capacitance of the coaxial cables connecting the system together is about 300 pf, so that special techniques must be used. In particular, the three wire circuit described by Hillhouse and Kline (1960) is fairly insensitive to the changes in the lead capacitance. A simplified schematic of the circuit used is shown in Figure 8 and the practical layout is shown in Figure 9. The circuit can be used to measure small capacitances in the presence of large lead capacitances because it makes use of the properties of a three terminal capacitor. The three terminal representation of a capacitor enclosed with in a metal shield is shown in figure 10. There are many bridge circuits which can be used to measure the direct capacitance of a 3-terminal capacitor, but most require separate bridges to balance the ground capacitance in the circuit. The ratio transformer capacitance bridge circuit in Fig. 8 is one circuit that does not require a secondary bridge.

Consider the circuit in Figure 11, where the ground capacitances The output impedance are shown. of the ratio transformer and the signal generator as seen by the bridge circuit is $5\,\Omega + 50\,\Omega S^2$, where S is the dial setting of the ratio

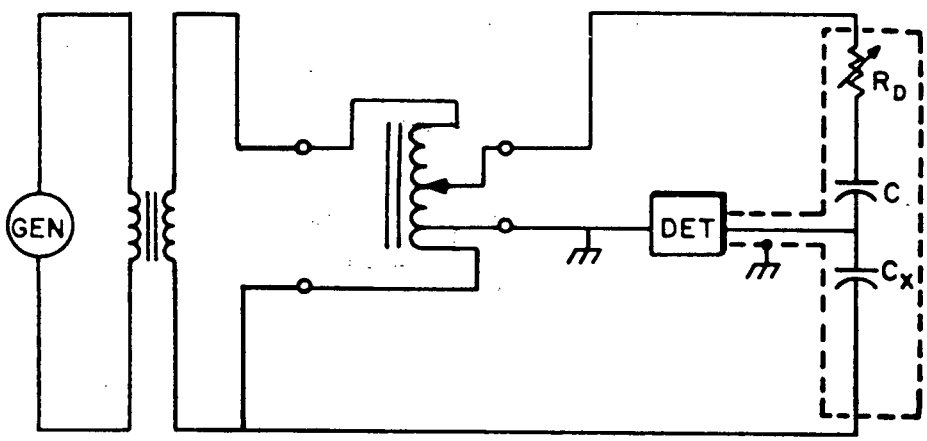

Figure 8. Schematic of the ratio transformer circuit. When balanced, $C_x = 10sC$, where s is the dial reading of the ratio transformer.

Figure 9. Capacitance bridge for the MCT.

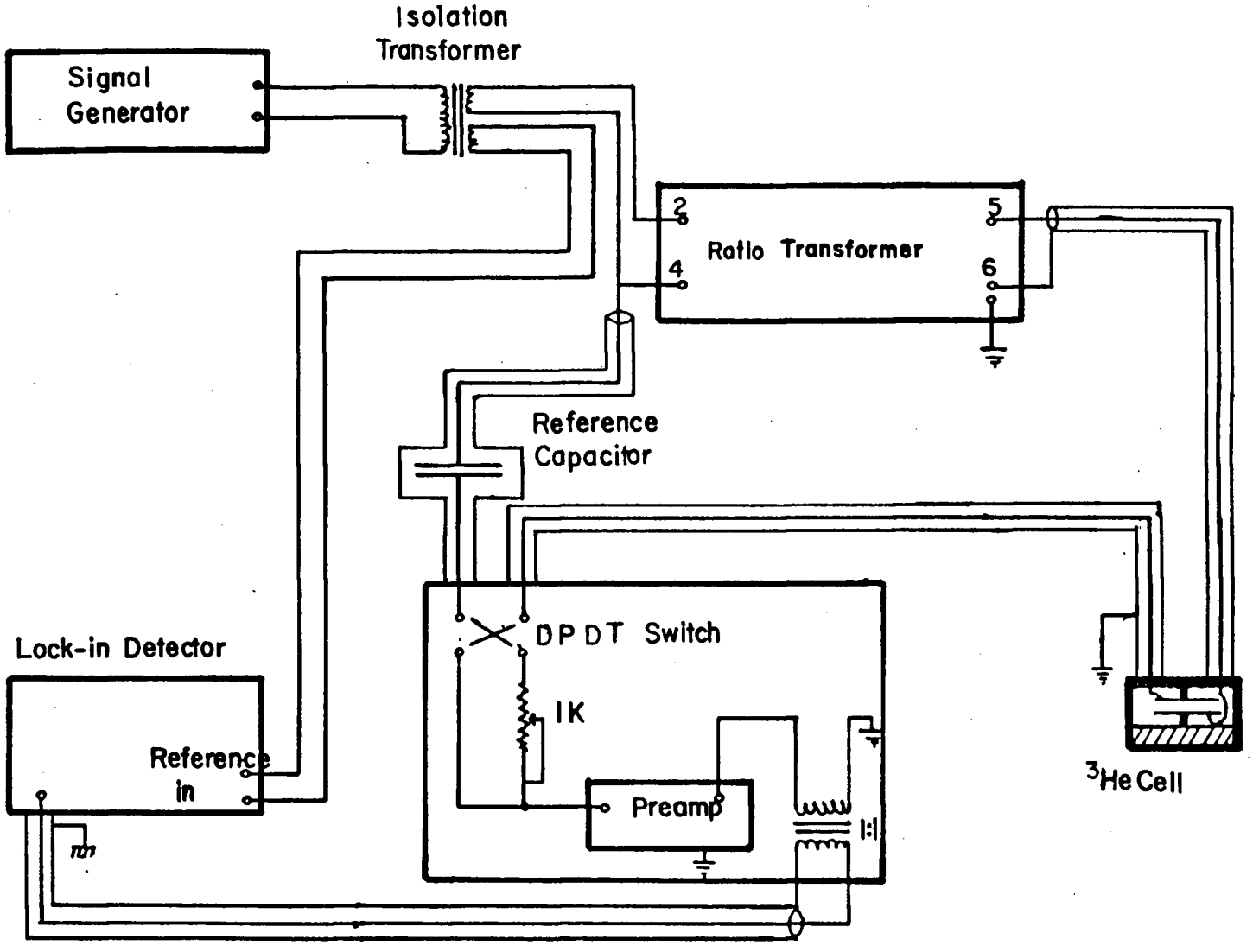

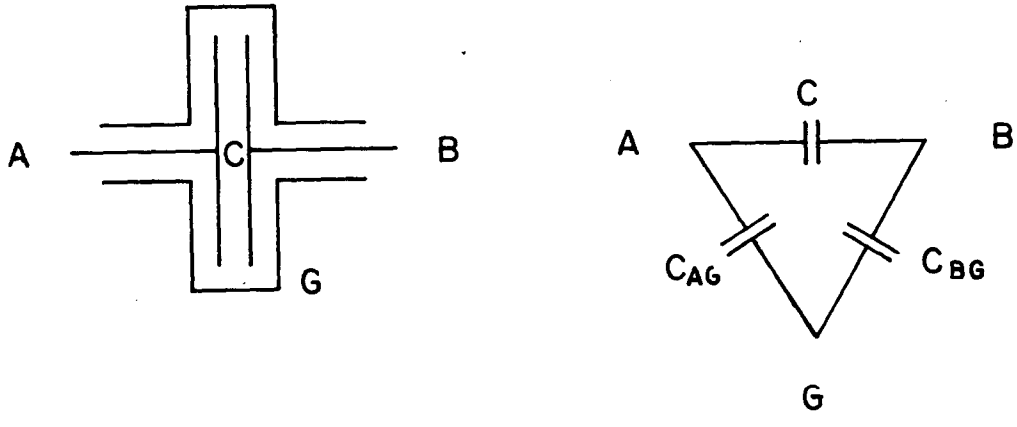

Figure 10. On the left hand side is a capacitor enclosed in a shield. On the right hand side is its schematic representation as a three terminal capacitor.

transformer. The output impedance of the bridge circuit is of the order of 1 Megohm, so that the ground capcaitance, C_g, is effectively shorted by the low impedance of the ratio transformer. The extent to which the capacitor, C_g, affects the bridge balance is found by considering the circuit in figure 12(a). The coupled inductor circuit is equivalent to the circuit in figure 12(b). The ratio of the voltage, E_1, across C_g, to the voltage applied, E, to the ratio transformer is given by

$$\frac{E_1}{E} = \frac{(L_2 + M) - \omega^2 C_g (L_1 L_2 - M^2)}{2M + L_1 + L_2 - \omega^2 (L_1 L_2 - M^2)(C_{g1} + C_{g2})}, \tag{49}$$

where $\omega = 2\pi f$. L_1 and L_2 are related to the coupling inductance M by

$$M = k\sqrt{L_1 L_2} \tag{50}$$

where k is a constant depending on the degree of the coupling between L_1 and L_2. If the inductances are coupled together so that there are no reactance losses, as in an ideal ratio transformer, k = 1, then ratio E_1/E is independent of the ground capacitances. In a practical ratio transformer, the coupling is very high(Kline and Hillhouse). An estimate of the error introduced by the ground capacitance is found by subsituting representative values for the ratio transformer used in the

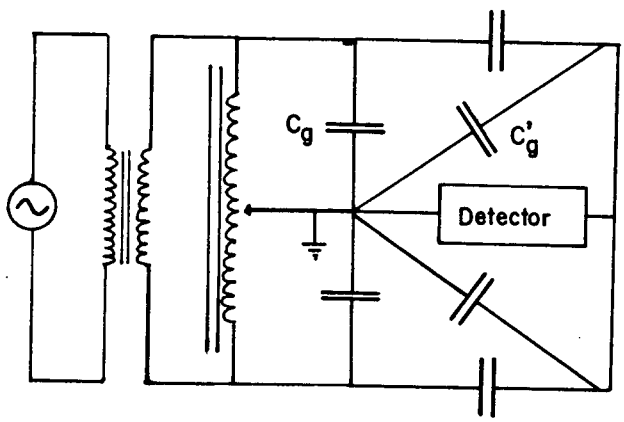

Figure 11. The ratio transformer bridge with three terminal capacitors.

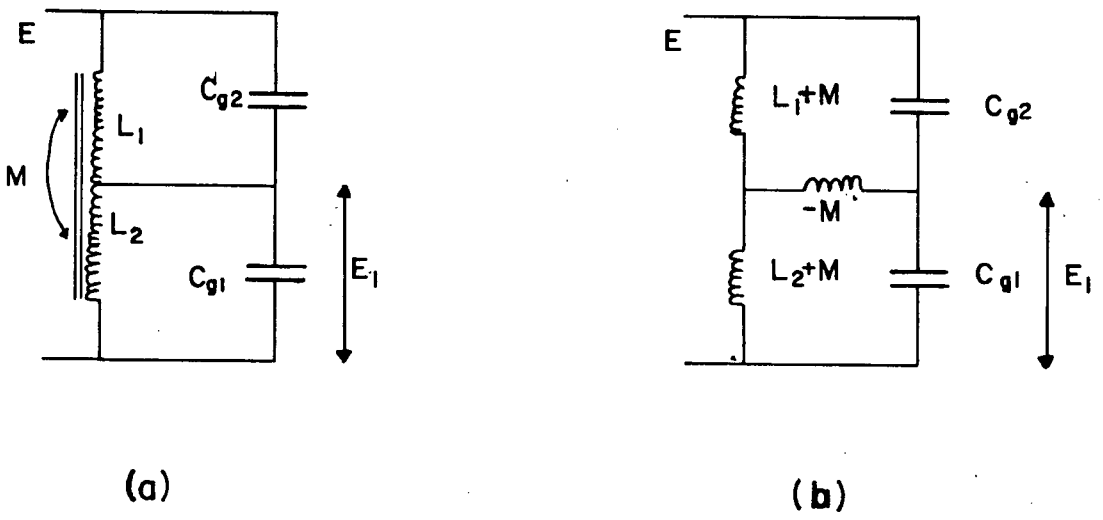

Figure 12. Schematic showing the ground capacitance(a) and the equivalent circuit of the combination of ratio transformer and the ground capacitance(b).

bridge: $L_1 = L_2 = 500$ H, $k = .999$, and the ground impedance is 100 pF. E_1/E is found to differ from 1/2 by 10 ppm. Thus the effect of the ground capacitance and $k = 1$, could be troublesome if an accurate measurement of a unknown capacitance were desired, but because the MCT requires only that the capacitance be measurable to a high resolution, this is of no real concern. In fact, because only a precise measurement in an arbitrary capacitance unit is required, the design of the bridge is much simpler than that of a bridge what must accurately measure the capacitance. The stray capacitances and inductances in the guard circuit shifts the balancing condition of the bridge, and thus shifts the measured capacitance value, but this shift is of no concern to a MCT, as long as the sensitivity is not reduced by them, and the shifts are reproducible.

It is vital that the leads to and from the reference capacitor and the ^{3}He cell be well guarded so that the capacitors approximate three terminal capacitors. The leads between the detector and the capacitors are the most sensitive to pick up and must be very carefully shielded. The bridge is insensitivity to drifts in the ground capacitance, but is sensitive to sudden fluctuations in the ground capacitance, which may introduce signals near the reference frequency driving the bridge.

The bridge used in the MCT circuit is driven by an HP 3330A Synthesizer, which has an 50 Ω output impedance, connected to a

1:1 isolation transformer in a sheet iron box, which is attached to the case of the ratio transformer. The transformer ensures that there is only one ground in the bridge circuit. There are two secondary coils on the isolation transformer, the signal from one is used as the reference signal for the HR8 PAR Lock-in amplifier. The second winding supplies the excitation voltage to an Electro Scientific Industries DT72A seven Decade Ratio Transformer, which at a frequency of 1 kHz is linear to 1 ppm. Most of the connecting cables in the circuit are RG-172U coaxial cables. However, the lead from the top of the vacuum can down to the ^{3}He cell is a Cooner AS636-1SSF coax, and the lead from the vacuum can to the tope of the cryostat is a semi-rigid stainless steel coax. It has been found that the semi-rigid coax is very noisy when cooled to liquid nitrogen temperature (i.e. vibrations induce electrical signals), whereas the RG-172U cable is almost unaffected by cooling. The drawback of the RG-172U is that it is poorly shielded and, thus requires additional braided shields to reduce the 60 cycle pickup.

The circuit for balancing the resistive component and the battery powered preamplifer are housed in an iron box to shield the system from 60 Hz magnetic noise.

The preamplifier uses a Siliconix U402 JFET, which has a very low gate leakage current and a reasonably low input noise voltage. The schematic diagram of the preamplifier is shown in Figure 13. The low leakage is required because at low

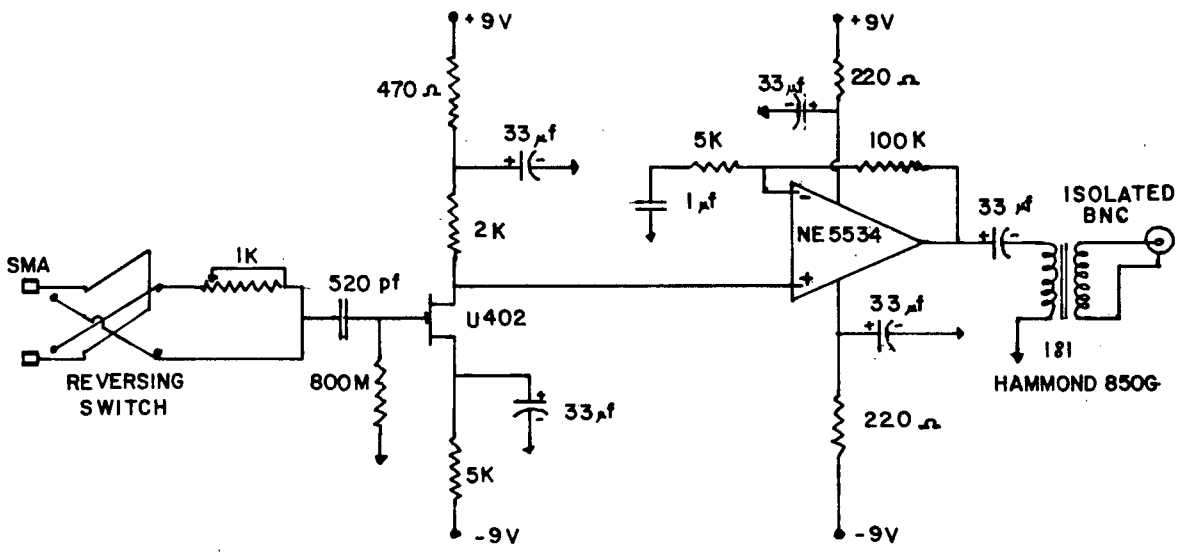

Figure 13. The high input impedance of the preamplifier reduces the Johnson noise current seen by the bridge.

frequencies the current noise is dominated by the shot noise of the gate current. The source impedance is essentially purely reactive and of order 0.5 Meg. This requires a very high value for the bias resistor(chosen to be 800 MΩ) if one is to avoid its Johnson noise. A NE5534 low noise operational amplifier which has a maximun input noise voltage of 4.5nv/$\sqrt{hz}$ at 1 kHz is used to amplify the signal by 228, before the signal is fed into the lock-in detector. The preamplifier is battery powered to decrease the number of ground loops in the system.

An 1000 Ω 10 turn potentimeter can be switched in series with either capacitor, so that the quadrature signal can be balanced.

The reference capacitor consists of a room temperature brass vacuum can which is connected by three 3/16" O.D. thick wall stainless steel tubes to a lower brass vacuum can. The top can has attached to it two hermetically sealed BNC panel mounts and a 1.5 lb relief valve. There are two separate compartments in the top can so that the leads down to and from the capacitor at the bottom are electrical independent. The whole assembly is evacuated. It was found that the bubbling of liquid nitrogen in contact with the coax can cause voltage pulses of several microvolts. The three s.s. tubes are silver soldered to the top and bottom cans. Two of the tubes each contain a RG-172U cable. The cables are pressed firmly against the inner walls of the the tubes by a string which is wrapped around the cables.

The immoblized cables are then fairly insensitive to microphonic pickup. All cables within the reference assembly are firmly clamped to the body of the assembly or to standoffs in order to prevent vibrations causing motion in the cables and thus inducing noise. The third tube is used as the pumping line to the bottom can.

The bottom can contains a 31.90 pf silvered mica capacitor. When it is cooled down to LN_2 temperature, its capacitance decreases by 0.10 pf. Because the reference capacitor is cooled by an open LN_2 bath, a stability in the capacitance of 1 ppm, requires that the atmospheric pressure must not change by more than 5 torr during the run. In fairly stable weather, there is a reasonable probability that the pressure will not change by more than 5 torr over the course of 1 to 2 days.

The change in the dielectric constant of the insulator in the coax, due to the change in temperature as the liquid nitrogen level in the bath falls, is not seen by the capacitance bridge because the ground capacitance changes slowly and by fairly small amounts.

3.6 Choice of Coaxial Cable for Low Temperature

It is a fact, perhaps not generally known, that electrical noise is generated in a coaxial cable when it is struck sharply. During the course of testing the reference capacitor assembly, it has also been found that most coaxial cables emit large amounts of electrical noise while they are being cooled (to liquid nitrogen temperature, for example). In some cases, the cables also became very microphonic. A brief study of the noise characteristics of coaxial cables that were available in the lab was conducted. The surprising result of the study was that the cheapest coax was the quietest and least microphonic of all the coax that were tested.

The cables that were examined are the RG 172, RG 142, RG 58, semi-rigid coax, and an "homemade" air dielectric coax. The "homemade" coax consisted of a length of 3/8" thick wall stainless steel tube with a shorter length of 1/4" thin wall stainless steel tube down the center of the larger tube. The inner tube was centered with four rings of expended ploystyrene insulation which were epoxied to the inner tube. One end of the 3/8" tube had a copper end cap soldered on. The other end had attached to it a BNC connector such that the center terminal could be soldered to the inner tube. After a rubber hose had been slipped over the BNC connector and the outer tube, a hypodermic needle was pieced through the hose. The air inside

the tube was displaced with helium that was forced in through the needle.

The noise in different cables was studied by attaching a length of cable to the input of the preamplifier used in the capacitance bridge and then observing the output on a 5440 Tektronic scope, which had it filters set to permit only D.C. to 10 KHz through. The opposite end of the coax was shielded to prevent the inner conductor from picking up the 60 Hz signal. Each particular cable was in turn tapped lightly with a plastic pen, whistled at, and finally, talked to , while it was at room temperature and then again at liquid nitrogen temperature. The results are summarized in Table II. The induced noise was measured by observing the maximum peak to peak signal produced in the cable.

Our conclusions are as follows. Coax cable at low temperature should not be exposed to boiling liquids, because electrical spikes as large as 100 mV can be induced in the cable. Thick or rigid cables in general are noisier than pliable cables at low temperatures. This may be due to the fact that the wires are more tightly wrapped in the thicker cable and therefore under more stress than the wires in the more flexible cables. Also, the better quality cables have teflon as the dielectric, whereas RG 172 has a softer ploye thylene dielectric. When picking a cable for low noise applications in the audio frequency range, one should choose a flexible cable with a

Table II

Peak to peak noise voltage in coax cables at different temperatures. The ambient room temperature values are a measure of the 60 Hz pick up of the cable. The ambient noise at low temperature is a measure of the ambient sound level in the room.

Coax	Room Temperature			Low Temperature (77 K)		
	Ambient (μV)	Tapping (mV)	Microphonic (μV)	Ambient (μV)	Tapping (mV)	Microphonic (μV)
"homemade" air core	18	0.4	7	6	0.13	13
RG 142	nil	9	nil	88	4	44
RG 58	9	4	nil	87	0.4	nil
Sem-rigid	nil	0.2	nil	13	13	13
RG 172	80	0.3	nil	80	0.2	nil
RG 172 shielded	nil	0.9	nil	nil	0.9	nil

non-teflon dielectric; one can reduce the electric pick up due to the poor outer braid by running the cable inside a conducting tube, for example, thin walled stainless steel tube.

IV. Thermometry with the Melting Curve Thermometer

4.1 Introduction

This chapter deals with the first use of the ^3He melting curve thermometer. As a test it was compared with a germanium resistor which had previously been calibrated against an SRM 768 fixed point device. The MCT was not directly compared with the SRM 768, because during the same run an experiment involving high magnetic fields was also conducted. It was felt that exposing the SRM 768 to a 40 kilogauss magnetic field might alter the calibration of the device.

A brief description of the procedure for operation the MCT is given the next section, a more complete description can be found in appendix A. The section following compares the temperature as measured by the MCT and the germanium device, and discusses the discrepancy in the measured temperatures.

4.2 Operating the MCT

Before the dilution refrigerator was cooled down, the ^{3}He was circulated through the cold trap to remove any impurities in the gas. The ^{3}He was then returned to the reservoir. The cell was pumped down with the charcoal pump so that there was only a few millitorr of the ^{3}He left in the cell. The ^{3}He in the cold trap was removed by pumping on the volume while the cold trap was still at liquid nitrogen temperature. The cold trap was then heated to 300 ^{o}C and pumped on with a diffusion pump for one hour. An analysis of the gas released by the molecular sieve indicated that most of the contamination was due to water, with traces of argon and nitrogen. The presence of argon gas was expected because the system had been pressure tested with it. The large concentration of water was attributed to the outgassing of the large ^{3}He reservoir.

During the cool down of the refrigerator, the capacitance of the ^{3}He tranducer was monitored with a Boonton capacitance bridge. At room temperature the capacitance of the cell was 3.15 pf. When cooled to liquid nitrogen temperature, the capacitance decreased to 2.622 pf, and at liquid helium temperature the capacitance of the cell was 2.574 pf. At this point the Sensotec transducer is measuring essentially zero pressure and the corresponding voltage output of the transducer is therefore the systematic zero shift, which must be taken into

account when using the calibration table supplied by the manufacturer.

When the refrigerator was functioning and maintaining a temperature of about 1 K, ^{3}He was compressed by the charcoal pump and slowly let into the cell through the cold trap at a rate of 0.01mV/sec on the Sensotec (about 0.2 psi per sec). To detect the presence of plugs in the capillaries, the capacitance of the cell was continually monitored with the Boonton during this process. After a pressure of 28 bars was reached, the transformer bridge capacitance was used instead of the Boonton meter. The bridge was driven at 980 Hz with a 15 dBm signal. About five digits could be usefully read from the bridge, because the fluctuations in the room temperature affected the gas pressure and caused fluctuations of 5 ppm per minute.. The pressure in the cell was increased to 34 bars and then decreased to 28 bars. The cell was exercised 5 times, during each cycle the capacitance of the cell was monitored as a function of the pressure. Between the third and fifth cycle a hysteresis of 0.1% was noticed in the capacitance at a given pressure. The time required for a pressure change to be transmitted between the cell and the transducer was very short. However, if large pressure changes (2 bar) were made, the relaxation time of the system at 30 bars pressure was about a minute.

Between the fifth and sixth run there was no measurable hysteresis, so cell was calibrated every 0.4 bars between

27.5 bars and 34.2 bars. In that region the equation

(51) $$P = 47.14429 - 36.957895\,s - 5.55361\,s^2,$$

where P is the pressure in bars and S is the dial reading of the ratio transformer, describes the calibration points with an error less than the uncertainty in the Sensotec calibration. Because the dilution refrigerator was running at a very high temperature, the temperature of each section was carefully monitored to ensure that the temperature at some part of the capillary did not drop below the freezing temperature during the pressure calibration.

The ^{3}He pressure was decreased to 33.9 bars and a ^{3}He plug formed in the capillary near the still, by increasing the pumping speed of the circulating system of the ^{3}He-^{4}He dilution refrigerator and so reducing the temperature at the still. The ^{3}He freezes at a temperature of 0.75 K (Grilly, 1871) at a pressure of 34 bars. When the still had cooled below 0.7 K, the pressure on the plug was increased to 35 bars to promote the growth of the solid plug into regions of higher temperature. The formation of the plug was verified by the fact that the ^{3}He cell showed no increase in pressure when the extra pressure was supplied.

The best starting density corresponds to pressures between 32 and 34 bars. The particular choice of the starting pressure

depends on the temperature range in which the MCT is to be used. To reach the lower temperatures, a higher starting pressure is required(Greywall and Busch,1982a). The location of the minimum pressure point is independent of the initial starting density for densities corresponding to pressures between 30.4 and 38 bars(Corrucinni et al., 1978).

The dilution refrigerator was then cooled to about 0.55 K, where the temperature of the mixing chamber was regulated. The capacitance bridge was nulled and the resistance of various carbon and germanium resistors was measured. A second point was taken at 0.5 K. It was then decided to take the temperature measurements while the refrigerator was warming up because it proved to be very difficult to maintain regulation at the higher temperatures while the refrigerator was on the cool down cycle.

The passage of the temperature through the minumum point on the melting curve was very noticable. It was possible, for example,to null the bridge to the 6th digit while the refrigerator was freely cooling.

The refrigerator would not cool down below 100 K, due to difficulties associated with the other experiment attached to the cryostat. There appeared to be a thermal short between the apparatus on the cold finger (attached to the mixing chamber) and the thermal shield, but because the thermometers being compared were all situated on the massive mixing chamber and the temperature was about 0.100 K, the resulting thermal gradients

are estimated to be very small.

From 0.1 K to the minimum pressure point, six readings were taken. About 15 minutes was required to regulate at a particular temperature. Because the sensitivity of the temperature regulator sensor increases at low temperature, the temperature was regulated to 0.05 mK around 300 mK, and to better than a few hundredth of milliKelvin at the lower temperature.

The thermal time constant of the thermometer at 300 mK was tested by measuring the pressure immediately after the temperature regulation was achieved at a fixed point, and then 10 minutes later. The two pressure measurements agreed to better than 4 ppm, indicating a thermal time constant of less than a minute for the system. The 4 ppm is a measure of the total drift in the system due to the drift in the regulated temperature, the drift in the capacitance bridge and the relaxation of the strain gauge. Unfortunately the thermometer was never cooled below 100 mK, so the thermal time constant at very low temperatures was not measured.

A second measurement of the minimum point was taken as the mixing chamber was slowly warmed up. The two measurements differed by only one in the sixth digit, this corresponds to a 0.03 mbar uncertainty in the precision to which the minimum was measured. The accuracy of this measurement, however, was only 0.05%, because the absolute certainty in the pressure

calibration of the ^{3}He cell is only 0.05%. Immediately after passing through the minimum pressure point the solid ^{3}He plug slipped and the cell was filled with solid ^{3}He. The plug slipped because the difference in pressure between the ^{3}He cell and the Sensotec transducer became too great for the plug to hold: after the plug had been originally formed, the pressure had been increased to 36 bars, but as the liquid helium level in the dewar fell, the pressure further increased. The difficulty can be remedied by decreasing the pressure on the plug before attempting to warm up through the minimum.

4.3 Comparison of the MCT with a Germanium Resistor

The MCT data consists of series of dial readings from the ratio transformer. These numbers are converted to a pressure by using equation (50). The minumum pressure measured by this MCT is 29.3067 bar 0.05%. The absolute uncertainty of 0.05% in the measurement is due to the Sensotec transducer and corresponds to 0.015 bar at this pressure. The established value of the minimum is 29.313 0.003 bars(Greywall and Busch, 1982a). The large number of figures in the MCT measurements was kept because the absolute uncertainty in the pressure measurements of the MCT can be decreased by shifting the pressure scale so that the measured pressure agrees with the accepted value. This amounts to assuming that the Sensotec suffers only from a systematic zero offset, which can be corrected. Because the Sensotec was calibrated with a dead weight tester accurate to 0.02%, the size of pressure units are probably good to 0.02%. Furthermore, because the diaphragm transducer gauge is ulitilized over only 10% of its full scale capacity, the gauge probably has a linear response curve over this region. A slight shift in the zero pressure point, therefore, decreases the uncertainty associated with the pressure calibration.

The reproducibility of the strain gauge and the stability of the capacitance bridge over a period of a day may be

questioned. However, given that the minumum pressure measured during the cool down cycle was within 3 ppm of the minimum pressure measured during the warming up cycle, the drift in the system is probably very small(on the order of 1 ppm per hour). Therefore the drift and reproducibitiy of the pressure measurement may be ignored to the precision of these measurements.

Two thermometers in addition to the MCT were attached to the mixing chamber. These were a Scientific Instruments germanium resistor(SI), Model 5-He3A, and a 400 Ω Matsushita carbon resistor (C). The carbon resistor had previously been calibrated against the SI. The SI had been calibrated with the SRM 768 and, also, with a Lakeshore germanium resistor, which in turn had been calibrated with a CMN susceptibility thermometer. Table III lists the results of the calibration run. The melting curve values given in Table II of Grilly(1971) was used as the calibration table for the MCT at temperatures above 0.318 K. A down shift of 2 mK was made in the temperatures interpolated from the graph drawn using the values given by Grilly to account for the 2 mK deviation of the T58 scale from the thermodynamic scale(see sec 4.4). The temperatures below 0.318 K were found by using the values given by equation (42).

Where the carbon resistance thermometer, C, is not decoupled from the system, the SI and the C are consistent in the temperature reading, but both measure temperatures which are

Table III

Temperatures measured by different thermometers,

S	Calculated Pressure (Bars)	Corrected Pressure (Bars)	MCT Temp. (mK)	SI		C	
				Resistance (Ω)	Temp. (mK)	Resistance (KΩ)	Temp. (mK)
.41538	31.3947	31.4040	589	2.22.6	589	1,845	589
.434474	30.8561	30.8645	550.	243.7	547	1.948	547
.467312	29.3067	29.3165	318			3.177	314
.434474	30.6315	30.6414	135.5	3.965 K	136	9.034	128
.441442	30.3518	30.3615	153.7	2.807 K	153	7.485	150
.446643	30.1425	30.1523	169.4	2.174 K	170	6.537	165
.455294	29.4926	29.5024	202	1.417 K	200	5.210	199
.466583	29.3363	29.3456	288	678.5	283	3.495	289

lower than the MCT measurements. Because the carbon resistor is located with a centimeter of the MCT, the possibility of thermal gradients in the mixing chamber can be ruled out. The SI readings deviates from the MCT temperatures by as much as 5 mK. It was noted that the SI has shifted its temperature curve at the higher end, where the agreement is the worst. The fixed calibration point device calibration of the SI in January 1983 show that, although previous calibration curves of the SI still agrees with the SRM 768 temperature at 99.02 mK and 162.6 mK, the SI curve has shifted by 2 mK to a lower temperature at the 205.7 mK point. If the SI calibration curve is shifted to agree with the fixed point temperature, then the MCT and the SI agree within a milliKelvin. It appears as if the SI needs to be recalibrated against the SRM 768, the Lakeshore, and the MCT.

The only real test for the MCT is to compare it with the SRM 768 and possibly the Lakeshore germanium resistor.

A small test of the accuracy of the MCT was to calibrate the C with the MCT and then the interpolated value of the resistance at 0.318 K was compared to the taken value of C measured when the MCT was passing through the pressure minimum. The two values differd by 1%, which corresponds to a 1 mK different at that temperature. Similiarly, if the SI is calibrated with the MCT, the fixed temperature at 205.7 mK from the January check is only 0.5 mK from the new curve. Although these fact do not confirm the validity of relying totally on the

MCT, they do instill some confidence in the MCT. As stated earlier, the only definitive procedure for checking the MCT is to compare its temperature scale with the SRM 768, the Lakeshore germanium, and hopefully a nuclear orientation thermometer at the very low temperatures.

4.4 Conclusion

A ^{3}He melting curve thermometer system has been built and tested. The pressure resolution of this particular MCT is 0.14 mbars. At temperatures less than 100 mK, this corresponds to an uncertainty of 7 μK. At the higher temperature of 300 mK, the precision is only 0.1 mK. With better temperature regulators and more calibration runs, it may be possible to decrease the estimate of the uncertainty in the pressure measurement. The absolute accaracy of the pressure measurement is determined by the room temperature pressure standard(which is 0.05%). With a uncertainty of 0.05% in the pressure measurement, the MCT can determine the temperature accurately to 0.5 mK at 50 mK and 1 mK at 260 mK. In fact, the accuracy in the pressure is somewhat better than 0.05%. The shifting of the measured minimum pressure to agree with the accepted value at that point, decreases the pressure uncertainty in the region where the highest accuracy is necessary, since near the pressure minimum, the temperature measured by the MCT is most sensitive to the pressure. As long as the pressure standard is reasonably linear around 29 bars, the shift in the pressure scale will decrease the uncertainty in the pressure measurement below 0.05%. If there were a large discrepancy between the measured minimum pressure and the accepted value, there might be some doubt as to the validity of rescaling the pressure. But,

because the determined minimum pressure is with its uncertainty of the accepted value, there is some confidence in the rescaling. Just how effective the shift is in reducing the uncertainty in the pressure is hard to determine. The only absolute method of checking the effectiveness of the pressure rescaling, is to do a calibration with primary temperature standards.

BIBLIOGRAPHY

1. Abel, W.R.; Anderson, A.C.; Block, W.C.; and Wheatby, J.C., Phys. Rev. 147, 111 (1970).

2. Anderson, A.C.; Peterson, R.E., Cryogenics 10, 430 (1970)

3. Anderson, A.C.; Redfield, A.G., Phys. Rev. 116, 583 (1959).

4. Anufviev, Y.D.; Peshkov, V.P., Soviet Physics, J. Low Temp. Phys. 34, 183 (1972).

5. Baker, G.A.; Gilbert, H.E.; Ever, J.; Rushbrooke, G.S., Phys. Rev. 164, 800 (1967).

6. Bargess, R.E., Proc. Symposium on the Physics of Superconductivity Reviews, University of Virginia, Charlottesville, Virginia (1967).

7. Berglund, P.M.; Collan, H.K.; Ehnholm, G.J.; Gylling, R.G., J. Low Temp. Phys. 6, 357 (1972).

8. Berman, R., Cryogenics 5, (1966).

9. Bloget, P.; Ghozlan, A.C.; Piejuc, P.; Sudvuund, M; Varoquanx, E.S.; LeFarr, D., Proc. on the 13th Int. Conf. on Low Temp. Phys., Plenum Press, New York (1973).

10. Brickledde, F.G.; van Dijk, H.; Duxieux, M.; Clement, J.R.; Logan, J.K., J. Res. N.B.S. A 64, 1 (1960).

11. Callen, H.B.; Walton, T.A., Phys. Rev. 83, 34 (1951).

12. Cameron, J.A.; Campbell, J.A.; Compton, J.P.; Glines, R.A.; Wilson, G.V.H., Proc. Phys. Soc. 90, 1077 (1967).

13. Corruccini, L.R.; Mountfield, K.R.; Sprenger, W.O., Rev. Sci. Instrum. 49, 314 (1978).

14. Dundon, J.M.; Stolfa, D.L.; Goodkind, J.M., Phys. Rev. Lett. 30, 843 (1973).

15. Durieux, M.; van Dijk, J.E.; ter Harmsel, H.; Rein, P.C.; Rusby, R.L., Temp. Control and Measurement 145, (1971).

16. Edertstein, A.S.; Mess, K.W., Physica 31, 1707 (1965).

17. Ganano, R. and Adams, E.D., Rev. Sci. Instrum. 41, 716 (1970).

18. Goldstein, L., Phys. Rev. 164, 270 (1967).

19. Goldstein, L., Phys. Rev. 171, 194 (1968).

20. Greywall, D.S. and Busch, P.A., Phys. Rev. Lett. 49, 146 (1982).

21. Greywall, D.S. and Busch, P.A., Rev. Sci. Instrum. 51, 509 (1980).

22. Grilly, E.R., J. Low Temp. Phys. 4, 615 (1971).

23. Halperin, W.P.; Rasmussen, F.B.; Archie, C.W.; Richardson, P.C., J. Low Temp. Phys. 31, 617 (1978).

24. Harrison, J.P., J. Low Temp. Phys. 37, 467 (1979).

25. Hirschkoff, E.C.; Symko, O.G.; Vant-Hull, L.L.; Wheatby, J.C., J. Low Temp. Phys. 2, 653 (1970).

26. Johnson, R.T.; Lounasmaa, O.V.; Rosenbaum, R.;Symko, O.G.;

27. Johnson, R.T.; Rapp, R.E.; Wheatby, J.C., J. Low Temp. Phys. 6, 445 (1972).

28. Kaluras, G.M.; Katila, T.E.; Lounasmaa, O.V., Mossbauer Effect Methodology, I. Gruverman, ed. (Plenum, London, 1969), Vol.5, p. 231.

29. Kammer, R.B.; Mueller, R.M.; Adams, E.D., J. Low Temp. Phys. 27, 319 (1977).

30. Kamper, R.A., Temperature: Its Measurement and Control in Science and Industry. 4, 349 (1973).

31. Kamper, R.A. and Zimmerman, J.E., J. Appl. Phys. 43, 132 (1971).

32. Kirk, W.P. and Adams, E.D., Phys. Rev. Lett. 27, 392 (1971)

33. Kittel, C., Thermal Physics, (John Wiley & Sons, Inc., New York, 1969).

34. Krane, K.S.; Murdock, B.T.; Steyert, W.A., Phys. Rev. Lett. 30, 321 (1973).

35. Krane, K.S.; Steffer, R.M.; Wheeler, R.M., Nucl. Data Tables II, 351 (1973).

36. Landau, J.; Tough, J.T.; Brubaker, N.R.; Edwards, D.O., Phys. Rev. Lett. 23, 283 (1969).

37. Landau, J.; Tough, J.T.; Brubaker, N.R.; Edwards, D.B., Phys. Rev. A2, 2472 (1970).

38. Legget A.J., Rev. Mod. Phys. 47, 331 (1975).

39. Marsh, J.D., Phys. Rev. Lett. 33A, 207 (1970).

40. Metrologia 5, 35 (1969).

41. Metrologia 15, 65 (1975).

42. Osheroff, D.D.; Richardson, R.C.; Lee, D.M., Phys. Rev. Lett. 28, 885 (1972).

43. Pratl, W.P.; Schermer, R.I.; Steyert, W.A., J. Low Temp. Phys. 1, 469 (1969).

44. Preston-Thomas, H., Meterologia 12, 7 (1966).

45. Richards, M.G.; Toffe, P.S.; Turner, P.R., Cryogenics 13, 182 (1973).

46. Richardson, R.C., Physica 90B, 47 (1977).

47. Roberts, T.R. and Sydoriak, S.G., Phys. Rev. 93, 1418 (1954).

48. Robichaux, J.E. and Anderson, A.C., Rev. Sci. Instrum. 40, 1512 (1969).

49. Roger, M.; Hetherington, J.H.; Pelrium, J.M., Rev. Mod. Phys. 55, 1 (1983).

50. Rose, M.E., Phys. Rev. 91, 610 (1953).

51. Rosenbaum, R.L.; Eckstein, Y.; Landau, J., Cryogenics 14, 21 (1977).

52. Rosenberg, H.M., J. Low Temp. Phys., Low Temp. Solid State Phys. (Clarendon Press, Oxford, 1965).

53. Scribner, R.A.; Panczyk, M.F.; Adams, E.D., J. Low Temp. Phys. 1, 313 (1969).

54. Silver, A.H.; Zimmerman, J.E.; Kamper, R.A., Appl. Phys. Lett. 11, 209 (1967).

55. Sites, J.R.; Smith, H.A.; Steyert, W.A., J. Low Temp.

Phys. 4, 605 (1971).

56. Sorelun, M.I., Noise, S.N.O.

57. Soulen, R.J. and Marshak, H., Cryogenics 20, 408 (1980).

58. Soulen, R.J., Physica 109-110, 2021 (1982).

59. Stephen, M.S., Phys. Rev. 182, 531 (1969).

60. Suomi, M.; Anderson, A.C.; Holmstein, B., Physica 38, 67 (1968).

61. Sydoriak, S.G.; Roberts, T.R.; Sherman, R.H., J. Res. N.B.S., G.B.A., 559 (1964).

62. Templeton, J.E. and Shirley, D.A., Phys. Rev. Lett. 18, 240 (1967).

63. Thouless, P.J., Proc. Phys. Soc.(London) 86, 893 (1965).

64. Trickley, S.B.; Kirk, W.P.;Adams, E.D., Rev. Mod. Phys. 44, 668 (1972).

65. van Dijk, H. and Durieux, M., Physica 24, (1959).

66. Webb, F.S.; Wilkinson, K.R.; Wilks, J., Proc. Royal Soc. (London) 214, 546 (1952).

67. Webb, R.A.; Giffard, R.P.; Wheatby, J.C., J. Low Temp. Phys. 13, 383 (1973).

68. Weinstock, H.; Lipschultz, F.P.; Kellers, C.F.; Tedrow, P.M.; Lee, D.M., Phys. Rev. Lett. 9, 193 (1962).

69. Wheatby, J.C., Rev. Mod. Phys. 47, 415 (1975).

70. Zimmerman, G.O.; Abeshouse, D.J.; Maxwell, E.; Kelland, D.R., J. Low Temp. Phys. 41, 79 (1980).

Apppendix A - Operating a MCT

The MCT consists of three separate systems: these are the pressure system, the capacitance bridge circuit, and the cell itself. When using this particular MCT, one must always remember a few important points. First, the pressure in the system must not excede 40 bars, except in the pump where 138 bars(2000 psi) can be stored safely. The cell should never be pressurized above 35 bars. Second, the thermistor gauge has an epoxy pressure seal, which should not be heated over 80 C. Third, when the MCT is operating the valve to the ^{3}He reservoir should always be left open so that the relief valve can function properly in the event of the refrigerator warming up. Finally, inappropriate opening of the valves to the vacuum line could result in a sizable amount of ^{3}He being lost.

Because the capacitance bridge has very high resolution, it is sensitive to many noise sources. First of all it is very sensitive to microphonics, and this is mainly associated with the preamplifier and the cables down into the cryostat. The noise introduced by microphonics can be reduced by damping the vibrations in the cables by rigidily supporting them.

The guarding connections on the coax must be continuous or large 60 Hz signals will be picked up by the inner conductors. The lock-in detector does not immediately filter out all of the beat frquencies between a multiply of the 60 Hz and the

reference frequency of the bridge, because the bandwidth of the bandpass amplifier is 50 Hz. Thus it is important that the driving frequency of the bridge be chosen to minimize the possibility of very low frequency beats which cannot be filtered by the output RC filters.

The ground of the bridge is through the cryostat. The lock-in ground is separate from that of the bridge to decrease the number of ground loops (This is possible because of the transformer output of the preamplifier).

The operation of the bridge is straight forward. With the lock-in detector on the least sensitive scale and using the largest decade knobs of ratio transformer, the output of the lock-in is zeroed. To converge to the correct setting, the zero is always undershot. Then the quadrature signal is nulled by switching the dissipation resistor into the approriate branch and adjusting the resistance to give a zero output. After verifying that the zero setting on the signal has not changed, one can continue onto the less significant figures of the ratio transformer. If adjusting the quadrature has shifted the null, then the procedure has to be repeated. As the setting gets closer to the null setting, the gain of the lock-in is increased appropriately

For the MCT, the dial reading need not be converted to a capacitance, rather, the pressure response of the transducer is related directly to the dial setting.

Before the initial filling of the system with ^3He, the system is pumped with an N_2 trapped diffusion pump for several days. Then the charcoal pump and the molecular sieve are cleaned by heating the pump and the cold trap to high temperature while still pumping on them. The cold trap is heated to 300 °C with the wire heater that is wrapped around the cold trap. The variac should not be turned aboue 45 volts or the heater may melt. The charcoal pump is warmed up by flowing warm air through the flow cryostat. Because there are soft solder joints in the flow cryostat the temperature should not be elevated above 100 °C. When the outgassing from the two containers has decreased to sufficiently low level, the two assemblies are sealed from the rest of the system. After the rest of the system is pumped down to less than a few millitorr, the vacuum line is shut.

With the cold trap at LN_2 temperature, ^3He is passed through the traps and then let into the reservoir. The pressure in the system is monitored with the Sensotec pressure meter. Two liters of ^3He at STP is required to pressurize the MCT. The main volume of the MCT is the reservoir with a 2.5 liter volume. When there is a sufficient quantity of ^3He in the tank , the valves to the ^3He reservoir and the ^3He supply are closed. When the pressure in the tubes is less than 10 millitorr, the valve to the charcoal pump is closed. The empty cold trap is now

heated to 300 ℃ to drive off the gasses on its surface and then pumped with a diffusion pump. It is then returned to LN temperature. The MCT is now ready to be used.

The Boonton capacitance meter is attached to the ^{3}He cell and the capacitance of the cell is monitored as it cools. The dilution refrigerator can now be cooled down.

With the refrigerator at 1 K, the ^{3}He is slowly loaded into the cell by slowly warming up the adsorption pump. The ^{3}He should flow through the cold trap and into the cell at a rate that increases the Sensotec reading by 0.01 mV/sec. All the main locations on the dilution refrigerator should be monitored to ensure that the refrigerator does not cool below 0.9 K. The pressure is increased to 34.5 bars. A record of the capacitance as a function of the pressure shold be kept so that the hysteresis in the cell can be observed. From 34.5 bars, the pressure is slowly decreased to 28 bars. This cycle is repeated four or five times. When the hysteresis has decreased to a value below the sensitivity of the Boonton meter, the capacitance bridge is connected to the cell. The cell will probably require about 5 cycles before the hystersis of the gauge is insignificant.

The calibration run consists of pressurizing the cell in 0.3 or 0.4 bar increments and measuring the cell capacitance at each point. The two valves leading to the cell form metal to metal seals at the seat and therefore, need to be firmly closed

or they will leak. The cell should be calibrated between 28 and 34.5 bars. The formula, $P = a + a S + a S^3$, is fitted to the calibration results. From 34.5 bars, the pressure is decreased to the plug forming pressure, and this can be anywhere from 30.5 to 34 bar on this MCT.

The circulation of the ^3He in the refrigerator is now increased to cool the refrigerator below the freezing point of the liquid. When the temperature is below freezing point, an over pressure of 0.5 bars is applied to promote the growth of the plug up the capillary. If the pressure in the cell increases, the plug is not completely formed. If this happens, the pressure is relieved to the original value and the refrigerator cooled further before the overpressure is applied. When the plug is completely formed, the MCT can be used as a thermometer.

The pressure on the top side of the plug increases as the liquid helium level in the dewar drops. The pressure must not be allowed to build up because the over pressure may cause the plug to slip. This is especially important when the MCT is slowly passing through the minimum. At this point, the pressure on the plug should be decreased to a few tenths of a bar above the pressure used to form the original plug and the temperature of the still checked.

At the end of the calibration run, the entire refrigerator should be warmed up to 1 K, so that the plug can melt and the

^{3}He slowly bled out into the reservoir through the cold trap. And finally, when the refrigerator is warming up to room temperature, the reservoir should be opened to the cell so that the pressure in the cell does not build up.